


Review

Collisions of Liquid Droplets in a Gaseous Medium under Conditions of Intense Phase Transformations: Review

Svetlana Kropotova and Pavel Strizhak * 

Scientific and Educational Department of I.N. Butakova, Power Engineering School, National Research Tomsk Polytechnic University, 634050 Tomsk, Russia; ssk22@tpu.ru

* Correspondence: pavelspa@tpu.ru

Abstract: The article presents the results of theoretical and experimental studies of coalescence, disruption, and fragmentation of liquid droplets in multiphase and multicomponent gas-vapor-droplet media. Highly promising approaches are considered to studying the interaction of liquid droplets in gaseous media with different compositions and parameters. A comparative analysis of promising technologies is carried out for the primary and secondary atomization of liquid droplets using schemes of their collision with each other. The influence of a range of factors and parameters on the collision processes of drops is analyzed, in particular, viscosity, density, surface, and interfacial tension of a liquid, trajectories of droplets in a gaseous medium, droplet velocities and sizes. The processes involved in the interaction of dissimilar droplets with a variable component composition and temperature are described. Fundamental differences are shown in the number and size of droplets formed due to binary collisions and collisions between droplets and particles at different Weber numbers. The conditions are analyzed for the several-fold increase in the number of droplets in the air flow due to their collisions in the disruption mode. A technique is described for generalizing and presenting the research findings on the interaction of drops in the form of theoretical collision regime maps using various approaches.

Keywords: liquid droplets; collisions; interaction regimes; secondary atomization; droplet breakup; combined atomization methods



Citation: Kropotova, S.; Strizhak, P. Collisions of Liquid Droplets in a Gaseous Medium under Conditions of Intense Phase Transformations: Review. *Energies* **2021**, *14*, 6150. <https://doi.org/10.3390/en14196150>

Academic Editors: Theodoros Zannis and Jaroslaw Krzywanski

Received: 30 August 2021
Accepted: 23 September 2021
Published: 27 September 2021

Publisher's Note: MDPI stays neutral with regard to jurisdictional claims in published maps and institutional affiliations.



Copyright: © 2021 by the authors. Licensee MDPI, Basel, Switzerland. This article is an open access article distributed under the terms and conditions of the Creative Commons Attribution (CC BY) license (<https://creativecommons.org/licenses/by/4.0/>).

1. Introduction

Liquid droplets are atomized in many applications. In particular, this technology is used for fuel injection into boiler furnaces or combustion chambers of engines, for cooling heat-generating components, as well as in heat and power units, gas turbines, and fire suppression systems. Droplet atomization usually comes in several stages. The first stage involves the so-called primary atomization by injectors. The second stage is used to increase the contact surface area of reagents and liquids, as well as to improve the efficiency and intensity of chemical reactions and phase transformations. This stage is about secondary atomization, which can be provided by intensifying various mechanisms and factors. Their choice depends heavily on the required concentration of the gas-vapor-droplet flow and average droplet size. With this in mind, special attention is paid to the thorough study of secondary droplet atomization in order to develop effective spraying technologies.

The most common secondary atomization methods are as follows [1–3]: droplet collision with an obstacle (meshes, frames, ledges, walls, substrates, rings, etc.); droplet collision with other droplets; droplet acceleration to high speeds and exceeding critical Weber numbers or an air jet impact on an aerosol; micro-explosive breakup or partial dispersion of heated heterogeneous droplets. The least energy- and time-consuming method is droplet breakup intensified by droplet collisions in a mist flow. Droplet interaction regimes are commonly classified into disruption, separation, bounce, and coalescence [4]. Separation is further subdivided into reflexive separation and stretching separation. Thus, it is sensible to study these collisions with varying liquid component compositions, velocities, droplet

sizes, mist flow concentrations, and ambient temperatures. The findings can be further used to adjust spraying systems. The use of two-step atomization reduces the time and energy expenditure for the generation of a gas-vapor-droplet flow with the required droplet size distribution. To provide high efficiency of the corresponding plants and units, a number of factors affecting such atomization is studied experimentally and numerically.

Today, droplet collision regimes and characteristics are studied using two approaches [2,5]: a phenomenological and a statistical approach. The former is based on recording the conditions, characteristics, and interaction regimes of two droplets (so-called binary droplet collisions). The latter involves the statistical analysis of collisions between liquid droplets as part of an aerosol. A reliable prediction of the corresponding processes will improve the efficiency of gas-vapor-droplet technologies, especially at high temperatures, which intensify changes in the composition and structure of gas-vapor-droplet mixtures.

The purpose of this review is to analyze and generalize the research findings on the use of four secondary atomization schemes: collisions of droplets with each other and with a solid wall, droplet exposure to an air jet, and micro-explosive breakup. Here, it is important to consider both the phenomenological and statistical approach to studying the conditions and characteristics of liquid droplet atomization.

2. Binary Collisions of Liquid Droplets with Each Other

A large amount of experimental and theoretical research data [3,5–17] in the field of droplet collisions has been accumulated as part of the phenomenological approach to studying binary droplet collisions. This approach is associated with fundamental research. It provides an opportunity to explore in detail not only the critical conditions of each droplet collision behavior but also the sizes, shapes, and velocities of post-collision droplets. This makes it possible to determine the optimal conditions for the contact surface area increase. One of the high-potential fields for the near future is the prediction of fuel droplet interactions in multicomponent and multiphase gas-vapor-droplet flows. Such research develops the ideas within the modern theory of droplet collision and coalescence, which serves as the basis for gas-vapor-droplet applications [10,17].

A review paper by Orme [5] contributed a lot to the understanding of binary droplet collisions. It generalizes the data published on the collisions of liquid fuel droplets as compared to water with a focus on collision outcomes. Orme tried to introduce a unified description of droplet interactions at the moment of collision and further motion of the resulting fragments. The detailed description of the possible outcomes of head-on droplet collisions classified into bounce, coalescence, disruption, and fragmentation was presented. The conditions of the occurrence of reflexive separation and stretching separation, which are also often singled out separate droplet collision regimes were described.

Collision outcomes depend heavily on the Weber number, the distance between the droplets' centers of mass, the surface tension and viscosity of the liquid, as well as the ambient pressure [5,6]. With this in mind, many scientists conclude that the research findings on droplet collisions can be conveniently generalized in the form of interaction regime maps in the $B(We)$ coordinates (Figure 1) and $We(Oh)$ coordinates [7,18]. Such maps determine the conditions, under which each collision outcome occurs. Thus, it is possible to choose the size, velocity, liquid properties, and impact angles of droplets so that their interaction led to their enlargement or atomization, depending on the required droplet size.

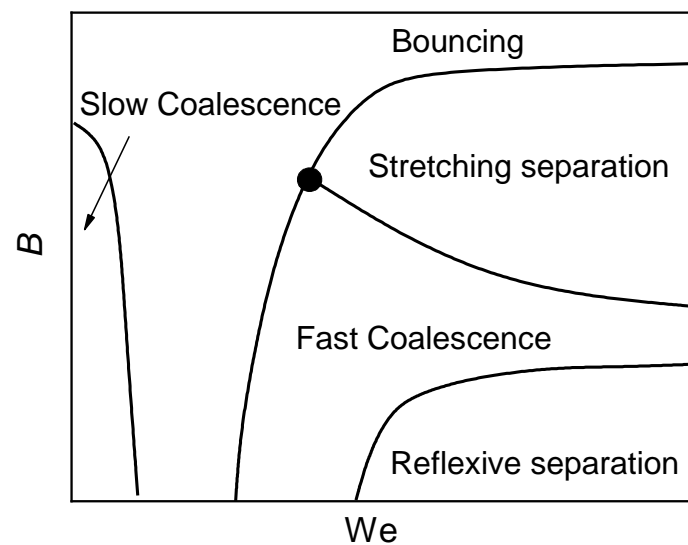


Figure 1. Droplet interaction regime map in the $B(We)$ coordinates, using the data from [18,19].

Two approaches are widely used in outlining the collision regimes when plotting an interaction regime map. The first approach distinguishes [2,5,7] four droplet collision regimes (Figure 2): bounce, coalescence, separation, and disruption. Bounce is notable for the elastic collision of droplets followed by their moving away from each other. The droplet surface remains intact and new droplets are not formed. During coalescence, the droplet surface disrupts at the point of contact, and two droplets merge into one large drop. In the separation regime, droplets merge and then separate without forming any new droplets. The disruption regime occurs when several secondary fragments are formed after parent droplets collide. In line with the second approach [2,6,7,16,18,19], five collision regimes are distinguished: fast coalescence, slow coalescence, bounce, stretching separation, and reflexive separation. The main difference between fast and slow coalescence is the duration of coalescence of parent droplets. Slow coalescence occurs when the Weber number is under 10. As part of reflexive separation, droplets coalesce and then break up into two to three child (satellite) droplets [16]. Stretching separation, also known as shift of layers, is notable for the formation of a liquid bridge between the colliding droplets, which then breaks up into a group of small fragments. Figure 2 also reports the location of the triple point, in which several interaction regimes can occur and which is often marked on regime maps [20,21].

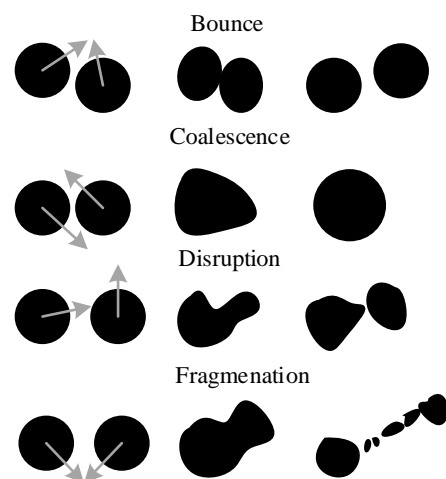


Figure 2. Typical droplet collision regimes described in [5].

Each of the above regimes occurs in a certain range of the Weber number. Droplet coalescence is typical of $0 < We < 0.5$ [8]. Droplet bounce occurs when the Weber number ranges from 0.7 to 1.5. Stable coalescence without a significant surface transformation occurs when the We numbers reach 2 to 15. When the Weber numbers fall within 15–50, droplet separation occurs. Droplet disruption into a large number of small fragments occurs when the Weber number exceeds 100. Zhang et al. described the criteria of occurrence for each regime [3]. They presented the equations describing the transition boundaries between regimes, Weber number ranges, droplet size ratios, and the distance between the droplets' centers of mass. A major contribution came from the findings presented by Pavlenko et al. [22]. They obtained analytical expressions describing droplet breakup characteristics. In particular, critical Weber numbers were determined using the critical diameter for unstable droplets and breakup times.

Several interaction parameters are generally used to describe droplet collisions [5,6] (Figure 3). The Weber number characterizes the correlation between inertia and surface tension. The Ohnesorge number accounts for the correlation of viscosity and surface tension. The parameter B describes the angular and linear droplet interactions. The parameter b characterizes the distance between the droplets' centers of mass. The impact angle α_d is measured from the line connecting the centers of mass of colliding droplets. Other interaction parameters include the relative droplet interaction velocity U_{rel} and the size ratio of colliding droplets Δ . In addition, when analyzing the efficiency of droplet atomization, it is sensible [9,11,12] to use the primary droplet to secondary droplet size ratio or the surface area ratio S_1/S_0 after and before the collision. The initial droplet surface area is derived from the sizes of the colliding droplets R_{d1} and R_{d2} : $S_0 = 4 \cdot \pi \cdot (R_{d1}^2 + R_{d2}^2)$. The surface area of secondary fragments is calculated by knowing their size and number: $S_1 = 4 \cdot \pi \cdot \sum N \cdot r_{di}^2$. Pavlenko et al. [23] expanded the above formula to factor in the probabilistic nature of the interfacial surface formation. They presented the following expression to determine the contact areas [23]: $S = \alpha \cdot N^{1/3} \cdot V_0^{2/3}$, where V_0 is the total volume of the dispersed phase and N is the number of spherical particles in the system. According to the authors, the total interfacial area depends on the volume of a medium and on the concentration of the dispersed phase. This parameter does not depend on particle size, but only on the law of their distribution, which is determined by the contact area ratio α . This approach is feasible for droplets colliding in a mist (within statistical approach described in the Introduction) rather than for binary droplet collisions.

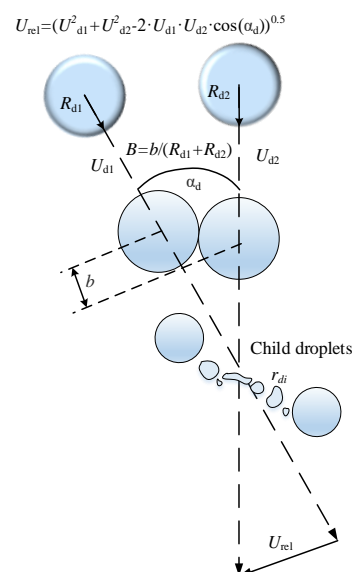


Figure 3. Droplet collision scheme used for experimental data processing (using the data from [12,24]).

Droplet size and velocity are among the technological parameters that need to meet certain requirements. The impact of these parameters on collision characteristics is studied in Refs. [13–15]. The sizes of colliding droplets as well as their ratio (Δ) are used to determine the boundary between regimes [3]. For instance, Orme [5] showed the impact of the droplet size ratio on their collision outcomes and the number of resulting fragments. Same-size droplets ($\Delta = 1$) collide to form several secondary (satellite) droplets, and the critical Weber number for the transient regime between droplet separation and coalescence is minimal at $\Delta = 0.7$ (for $Re = 600\text{--}4000$). Zhang et al. [3] presented the experimental findings on droplet coalescence and separation after their collision accounting for the impact of droplet size. The size of droplets ranged from 0.5 mm to 2.5 mm. Zhang et al. [3] also determined the influence of the dimensionless ratio of droplet length to its width on droplet collision behavior. This dimensionless parameter is minimal for separation and maximal for coalescence. These findings are valuable for the technologies that require an increase in the free surface area of liquid fragments and an improvement of fuel combustion efficiency without significant energy expenditures. Refs. [13–15] determined the droplet sizes, velocities, and impact angles that provide the conditions for the above requirements. It was established that the parameters obtained can be used for adjusting the atomization systems to provide rapid droplet disruption through their collisions.

In the field of liquid atomization in a gas–vapor medium, droplets are commonly classified on the basis of their role in the collision process [4,25]. Larger droplets are commonly called targets and smaller droplets are known as projectiles. A target droplet has a lower velocity as compared to a projectile droplet, or it may even be sessile in the experiments. This approach makes it possible to choose the collision parameters so that droplet atomization could require minimum energy. It is also used for collisions of immiscible droplets. For instance, Planchette et al. [4] studied the collisions of immiscible liquid droplets as a promising method of providing droplet encapsulation with a preset film thickness. The classification of droplets into a target and a projectile is of special importance when a droplet free-falls on a liquid film or on a sessile droplet sitting on a surface [26] (such processes occur when droplets are supplied to a surface to cool it down). Piskunov et al. [25] distinguished the differences between the breakup of target and projectile droplets colliding with each other. They established that a target droplet breaks into a much larger number of secondary fragments than a projectile droplet in the Weber number range of 50 to 150. Planchette et al. distinguished crossing separation as a separate collision regime of immiscible droplets, in which secondary droplets are only formed out of one liquid [4]. This makes it possible to distinguish between secondary fragments formed from the breakup of the projectile droplet and target droplet.

Research findings on the impact of the viscosity, density, and surface tension of liquid on the characteristics and outcomes of droplet collisions became widely known [4,6,21,27–29]. Sommerfeld et al. [27] proposed a model describing the critical values of the Weber number (We) for the boundaries between reflexive separation and stretching separation. They found a point on the regime map in which bounce, coalescence, and stretching separation may occur depending on the viscosity. An increase in the liquid viscosity was found to result in a shift in the position of this point towards the smaller dimensionless linear interaction parameter (B). Interesting results were obtained as part of research into the impact of interfacial tension of liquid on the integral characteristics of droplet collisions [28,29]. Refs. [28,29] studied emulsions based on silicone oils with an interfacial tension ranging from 0.0229 to 0.0505 N/m. They analyzed the impact of interfacial tension of liquid on the duration of droplet coalescence. It was experimentally established that the impact of interfacial tension is only observed in the range of low flow velocities (under 10^{-2} m/s). Gao et al. [30] outlined the effects of velocity fluctuations on liquid spraying and droplet deformation in an aerosol. They established that a transition from laminar to turbulent flow causes greater droplet deformation, and more droplets collide at random with a decrease in surface tension.

Many industrial applications make use of collisions between droplets with different viscosities [12,31–33]. An important stage in the fundamental research of such collisions is the study of similar-size droplets colliding with each other with various degrees of off-centeredness. The dynamics of such collisions were studied by Focke et al. [31]. They explored the collisions of highly viscous (25% Polyvinylpyrrolidone solution) and low viscous (5% Polyvinylpyrrolidone solution) liquids to establish that an increase in the viscosity of one of the droplets significantly slows down droplet coalescence (the coalescence time reached 1700 μ s). Tkachenko et al. [12] recorded the fluorescence of two parent droplets and the droplet that resulted from their coalescence. They established the deformation characteristics of the near-surface layer of two colliding droplets, the liquid mixing speed, and the time of complete mixing after coalescence. Research in this field makes it possible to analyze the liquid distribution inside each of the droplets as a result of their collisions, which is especially important when studying dispersed two-phase flows [12].

Baumgartner et al. [33] investigated the impact of the viscosity of liquid on the outcome of a collision between immiscible droplets and jets. In particular, they focused on collision outcomes, when a droplet collided with a jet to deform into a curved plate with a rim formed around it. An increase in viscosity was found to cause a significant stabilization of droplets and jets. The maximum droplet deformation inside a jet was shown to depend solely on the impact velocity and droplet viscosity. The authors conclude that the parameters of collisions between droplets and jets can be modeled using Weber and Reynolds numbers.

Shlegel et al. [34] plotted interaction regime maps accounting for the Weber and Ohnesorge numbers to factor in the properties of liquid. They studied the impact of liquid viscosity as well as surface and interfacial tension on the number and size of secondary droplets. It was shown that a 50% decrease in surface tension led to a 50–65% decrease in the Weber numbers required for droplet breakup into a group of small fragments. At the same time, a two-times increase in viscosity only increased these values by 5 to 15%. The experimental findings [34] suggest that, by selecting the viscosity, density, and surface tension of a liquid in certain ranges, one can control the intensity of droplet breakup into a cloud of small fragments.

The results obtained in Refs. [3,5–15,17,35,36] contribute to the development of chemical and petrochemical technologies based on collisions of single-component and multicomponent droplets as well as gas-vapor-droplet technologies. In addition to liquid properties, a significant impact on droplet interaction regimes comes from the characteristics of the gaseous medium in which collision takes place (for instance, temperature, humidity, pressure [37], etc.). This happens because these parameters are not at all standard in the technological equipment. Droplets are exposed to a range of forces, so they transform significantly, collide with each other, and are more likely to explode; droplet size distributions are constantly changing. Research findings obtained in this field provide a deeper insight into droplet collisions. In particular, Strotos et al. [38] presented the simulations of droplet breakup (in the Weber number range of 15–90) in a gaseous medium heated to high temperatures (150–700 °C). It is shown that the Weber number is the controlling disruption parameter, while the Reynolds numbers affect droplet breakup in the low We range. At the same time, although heating significantly reduces the surface tension of liquid, the overall hydrodynamic behavior of droplets (transformations, breakup intensity, and the nature of secondary droplet formation) does not change much. Strotos et al. [38] link this to the short duration of droplet heating in a gaseous medium and to high volatility of the fuel under study. The heating of the gaseous medium affects droplet collision mostly at low Weber numbers and with a significant difference between the liquid and gas temperatures. Droplet collisions under high pressure were modeled by Dupuy et al. [39] for the conditions of real industrial application (as illustrated by a scrubber). They analyzed the coalescence process under high pressure of the gaseous medium. The research findings are of special importance for selecting the parameters of equipment operation in which droplets collide under high pressure and can be used to predict the improvement of industrial performance.

Dupuy et al. [39] hypothesize that it is sensible to use the Reynolds number rather than the Weber number to describe droplet collisions in a gaseous medium under high pressure. Qian et al. [18], in turn, showed that the pressure of the gaseous medium affects the boundaries between regimes in the $B(We)$ maps. They established that droplets mostly coalesce and bounce at atmospheric pressure (up to 0.7 atm). When the pressure goes up to 4.4 atm, separation and disruption occur. The Weber number at the bounce–coalescence boundary increases significantly with an increase in pressure.

In Ref. [35], the authors experimentally studied liquid droplet collisions in a heated gas. They showed the impact of the gas temperature as well as droplet size and velocity on droplet bounce parameters. It was established that the bounce regime occurs at low resultant droplet velocities and at a gas temperature of about 20 °C. When the gas is heated up to 80 °C, the droplet bounce occurs several times as frequently, which results from the intense evaporation of small droplets and the formation of a buffer layer around them. The formation of this layer was also observed by Kuznetsov et al. [40] during the collision of two water droplets heated up to 90 to 95 °C. The thickness of the vapor layer was 12–18% of the diameter of the resulting droplet formed by coalescence [40]. In turn, Tkachenko et al. [37] showed that the critical Weber numbers decrease by a factor of 10–30 with a temperature increase from 20 °C to 200 °C.

In their theoretical research [7], Krishnan and Loth controlled for the impact of liquid viscosity as well as pressure and density of the gas medium on the spraying characteristics. They established that these parameters are of special importance in fuel systems with jets under pressure. An increase in the viscosity of colliding droplets and in the gas pressure was found to result in higher probability of droplet bounce [7].

In addition to liquid droplets colliding with each other, researchers focus on droplet interaction with solid particles. This is a promising field of production processes, because such interactions are encountered in many applications involving solid particle capture by droplets, for instance, in spray drying and water treatment. The key research in this field deals largely with droplet and particle size distribution in a two-phase flow. Research by Gac and Gradoń [41] showed that the duration of droplet/particle collisions depends on their size ratio, and the collision regime depends on the Weber number. Droplet shape has no real impact on collision characteristics. Pawar et al. [42] classified droplet interaction outcomes into agglomeration (the particle sticks to the droplet) and separation of the particle and the droplet with the formation of secondary droplets. The impact of hydrophilic and hydrophobic behavior of particles on collision regimes was studied by Yang and Chen [43]. They showed that when particles are hydrophobic, droplets bounce off them, whereas a hydrophilic particle passes through a droplet, which breaks up into secondary fragments. Malgarinos et al. [44] theoretically described droplet/particle collisions in the injection zone of a fluid catalytic cracking reactor in the temperature range of 205 to 400 °C. Collisions were simulated using a three-dimensional model of a two-phase CFD flow. The authors studied how droplet size and particle temperature affected droplet–particle interaction. As droplets moved between catalytic particles, a thin liquid layer was formed and droplet levitation was observed due to a vapor layer between particles.

Yoon and Shin [45] established that despite the vast amount of research into collisions between droplets and particles, some points were still neglected. In particular, the focus is usually on narrow ranges of parameters for such collisions (the behavior of a particle colliding with liquid with differing characteristics is still understudied). With this in mind, the authors explored the maximal spread of a droplet following its collision with a dry sessile spherical particle in a wide range of the Weber number (30–90), Ohnesorge number (0.0013–0.7869) and droplet/particle size ratios (1/10–1/2). They presented an empirical correlation applicable to droplet collisions with both a particle and a flat surface.

The research findings described above serve as the database that can be used to design fibrous filters and optimize liquid treatment technologies. Furthermore, we present the research findings in the field of gas-vapor-droplet applications obtained using the statistical approach (jets and mist flows). This approach requires greater time and energy expen-

ditures as well as the use of expensive equipment (optical systems recording hundreds of droplet collisions simultaneously). However, the research findings obtained using this approach are representative of real technologies.

3. Collisions of a Large Array of Droplets

In the industrial technologies described in the first section, droplets mostly move and collide in the turbulent regime, where droplet concentration in a flow is high and droplet size varies in a wide range (10–1000 μm). The analysis of the theoretical findings and conclusions shows that the initial parameters of the vapor–liquid medium, in particular temperature, particle size, and content of additives, play the decisive role in forming the gas-vapor-droplet flows. Here, it is sensible to study droplet collisions in a mist, controlling for a set of factors that are typical of technological systems and equipment: concentration and velocities of droplets as part of a mist, pressures of spraying systems, temperatures, etc. There has been a number of interesting studies in this field, whose findings can be used in real industrial technologies. In particular, the impact of the injection pressure P (in the range of 12–20 bar) on droplet collisions was studied by Santolaya et al. [46]. They used industrial oil heated to 95 °C as the liquid under study. It was shown experimentally that an increase in the pressure P from 12 to 20 bar improves the spraying characteristics. For all the pressures, the liquid spatially redistributed after jet disruption largely due to droplet interaction with the air flow. Droplet velocities were measured to find that velocity variations along the flow increase the intensity of droplet collisions. As a result, they coalesce, and the average droplet diameter increases.

The average Weber numbers and droplet collision frequency increase significantly with an increase in the liquid discharge pressure. Here, head-on droplet collisions are the most frequent ones leading to the formation of secondary fragments. Modified bio-diesel was sprayed at high ambient pressures (100 and 300 bar) as part of experiments by Ghahremani et al. [47]. An increase in ambient pressure was found to increase the jet angle and the liquid spray area. With an increase in the injection pressure, the Reynolds number increases due to more intense turbulent fluctuations. Ghahremani et al. [47] established that an increase in this parameter together with a rise in Oh improves spraying efficiency.

The impact of injection pressure of bio-diesel on its spraying characteristics was studied by Ghahremani et al. in Ref. [48]. The authors established that even a slight increase in the injection pressure or percentage of diesel fuel in a blend may significantly increase the jet angle and hence the spraying area. At the same time, one of the key ways to improve spraying efficiency is by increasing the difference between the injection pressure and the ambient pressure. Spraying characteristics can also be maintained by a simultaneous increase in the Ohnesorge number and decrease in the Reynolds number. Spraying can be characterized using the Sauter mean diameter [48]. Sauter diameter is the diameter of a droplet that has the same volume/surface area ratio as the entire array of droplets in a jet. The Sauter mean diameter calculated by Ghahremani et al. [48] with varying ambient pressure and injection pressure is given in Figure 4 for various types of fuel. Figure 4 shows that an increase in the injection pressure and ambient pressure improves the fuel jet spraying efficiency.

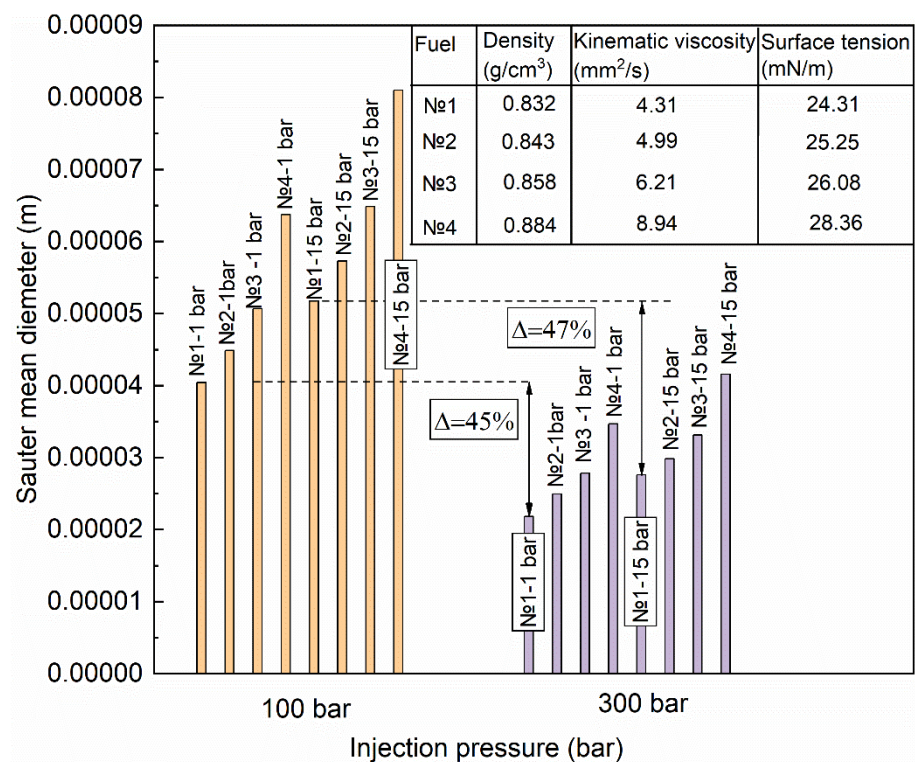


Figure 4. Variation of Sauter mean diameter with an increase in the injection and gas pressure (comparison using the data from [48]).

The widely used diesel fuel has high combustion efficiency and stability parameters. However, there are environmental downsides to its use. That is why emulsified fuels, which improve combustion efficiency and reduce air pollution, are generating a considerable interest as a subject of research [49,50]. Ismael et al. [50] showed that injection pressure has a significant impact on the secondary atomization of a water-in-diesel emulsion. In particular, at high injection pressures (500, 1000, and 1500 bar), water evaporation leads to puffing and micro-explosion [50]. The properties of emulsion (size and number of dispersed droplets) change after injection, and the water evaporates rapidly due to high pressure and temperature. As the authors showed, the injection time depends more on the size of dispersed droplets and water content in a droplet than on the original droplet size in a spray flow.

The key parameter of a mist flow is its size distribution, which reflects the volume concentration of droplets in a gaseous medium. This parameter characterizes the liquid consumption and the average droplet size in a flow. To improve the performance of gas-vapor-droplet units in heat and mass transfer applications, it is important to control droplet concentration in a gaseous medium [51]. However, this parameter is rather difficult to predict, because mist flows from several nozzles are mixed together. Due to the difficulty of technical implementation, there is not enough experimental research on droplet collisions in a mist flow. Not many research findings [52] are available on the impact of droplet concentration in a spray flow on droplet evaporation characteristics in gaseous media heated to high temperatures. Ref. [52] shows that this impact may be significant even in the medium temperature range.

Vysokomornaya et al. [53] experimentally studied droplet collisions in a spray flow. They explored the impact of liquid flow turbulence on droplet collisions. The outcomes of such collisions were described using the We and Re numbers, which varied in the range of 1100 to 2800. The occurrence probability was calculated for each regime. It was established that higher flow turbulence rate (provided by increasing the Re numbers) increases the intensity of droplet interaction. As a result of such interactions, droplets may bounce,

coalesce, or break up. Intense atomization or the enlargement of droplets can be provided by setting the spray nozzles at an optimal angle. The regime occurrence probabilities depending on the Weber and Reynolds numbers calculated by Vysokomornaya et al. [53] can be used to predict the flow structure for heat exchange equipment and fuel technologies.

In practical applications where it is necessary to intensify the evaporation of spray droplets (for instance, in direct-contact heat exchangers or polydisperse firefighting systems), it is advisable to reduce the volume concentration of droplets. This can be done by varying the liquid flow through injectors as well as by decreasing the injection pressure and rate. An interesting result in this field was obtained by Volkov et al. [54] using high-speed video recording, Tema Automotive software, and panoramic optical techniques (PIV, Stereo PIV, PTV, IPI, SP). They obtained the characteristics of 100–300- μm droplets moving in a reversed flow of gases heated to about 1100 K. Droplet concentration was varied in the wide range [54], which is typical of numerous practical applications in gas-vapor-droplet technologies. In the course of experiments, the authors determined the integral characteristics of droplet evaporation (in particular, mass vaporization rates). With an increase in the volume concentration of droplets in a liquid flow, their evaporation was shown to slow down in the area of high-temperature combustion products. It was established that the mist flow covering 1 m in a high-temperature gaseous medium induces a 70–95% decrease in the volume concentration of droplets. This was linked to the intense evaporation of droplets under 100 μm [54]. The findings can be used for predicting the conditions of droplet evaporation in a mist flow with varying droplet concentration in a wide range.

In practice, secondary droplet atomization is often provided not only by setting the parameters of atomization systems but also by mixing liquid flows from two injectors (nozzles) installed at an optimal distance at different angles to each other. This nozzle layout provides the intersection of spray cones, which significantly increases the probability of droplet collision and intensifies their atomization. In this case, the droplet breakup rate depends greatly on the collision angle and We numbers, as well as on the liquid viscosity, density, and surface tension. The main focus here is on increasing the number of secondary fragments formed due to collisions of parent droplets and on studying the effect of the above parameters [55,56]. For instance, interesting patterns in diesel aerosol intersection were analyzed by Almohammed and Breuer [57]. They studied the mixing of flows generated by two injectors positioned at 90° to each other at a distance of 0.07 m. As shown, due to such nozzle arrangement, the greatest number of droplet collisions occur in the area of flow intersection leading to droplet coalescence. The droplets formed by this coalescence are almost four times as large as the pre-collision droplets (droplet size after primary atomization is 175 μm , and it is 400 μm in the droplet flow intersection area). It is advisable to use the model developed in Ref. [57] for the numerical investigation of droplet coalescence in real applications.

Ruan et al. [58] explored the intersection of two spray flows under different operating conditions and the impact of flow velocities and collision angles on this process. The intersection angle of mist flows makes the greatest contribution to the breakup process. The impact of the flow velocities was determined using the Weber numbers, which ranged from 30 to 10,373. The research findings show [58] that at low We numbers (and, hence, low resultant velocities), the collision of liquid flows does not lead to the intense disruption of droplets colliding in the area of their intersection. The liquid jets are stable and have an ellipsoidal shape. Higher velocities (increase in the Weber numbers above 200), however, intensify the disturbances and lead to the intense jet disruption into a fine mist.

Fathinia et al. [59] presented their research findings on the performance improvement of spray flash evaporation desalination systems. Nozzles with a flow rate of 2–17.8 L/min were arranged at 30–60 mm from each other at an angle of 65°. The injection pressure ranged from 0.25 to 6 bar. The temperature of the gaseous medium was 70 °C. The research findings [59] show that an increase in pressure from 0.25 to 6 bar has a negligible effect on the volume of the evaporated water (no more than 1.05 L). A significant impact on this

parameter comes from the nozzle arrangement. The maximum performance improvement is 28% when the nozzles are at a maximum distance from each other.

Studies of collisions between droplet flows and particles occupy a special niche in the research of droplet flow interactions [51]. This field holds some potential, but there are not enough numerical and experimental data in this area to develop a theory. This is generally linked with the difficulty of technical implementation of such experiments. The collision outcomes of droplets in a mist obtained by the statistical approach serve as a database to predict droplet collision parameters with varying spraying parameters (relative droplet concentration in a gas as well as gas pressure and temperature) in a wide range. The analysis of these factors provides a deeper insight into the structural and compositional changes in gas-vapor-droplet flows as part of real technological equipment.

4. Liquid Droplets Colliding with a Solid Wall

Droplet disruption after colliding with a solid surface is implemented in a wide range of industrial applications (fuel injection into combustion chambers, desalination, cooling, heat transfer in evaporators, water droplets hitting turbine blades, etc.). Research in this field focuses mainly on droplet interaction with a solid surface and with a surface covered by a liquid film. Today, an extensive body of experimental research findings has been accumulated on the effect of surface properties (roughness, hydrophilic and hydrophobic behavior, heating, and slope) on droplet collision dynamics. Review papers [60,61] made a significant contribution to the research into collisions of liquid droplets with surfaces. Liang and Mudawar [60] focused on high-velocity droplet impingement on a solid surface, spreading over it and forming a liquid film, as well as a crown with small secondary droplets shattering from the crown's rim. The mechanism of this interaction is shown in Figure 5. The main factors affecting the droplet impact dynamics are generalized and distinguished [60]: droplet size (diameter), impact velocity, temperature and liquid properties (viscosity, density, and surface tension), and the surrounding gas properties (pressure, temperature, density, etc.). Liang and Mudawar outline the mechanisms for determining the characteristics of a liquid film with the specified roughness range of the wall and impact characteristics [60]. They also describe the crown formation dynamics with the specified Weber numbers, film thickness, diameter, and height, as well as droplet velocities, at which the crown is formed. It is shown that with $L_{nd} < h^* < 3 R_{nd}^{0.16}$ (where h^* is the non-dimensional film thickness, R_{nd} denotes the non-dimensional wall roughness parameter, and L_{nd} refers to the non-dimensional length scale of wall roughness), the Impact depends on wall features. In the range of $3 R_{nd}^{0.16} < h^* < 1.5$, the liquid film regime occurs, and the Impact is weakly dependent on wall features. For the shallow pool regime, the range of these parameters is $1.5 < h^* < 4$: In this case, the Impact depends on film thickness but is independent of wall features. In the deep pool regime ($h^* > 4$), the Impact is independent of film thickness.

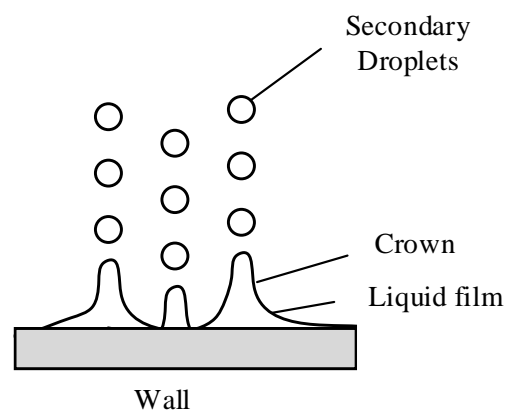


Figure 5. Mechanism of secondary droplet formation.

A large number of secondary droplets are formed when a droplet collides with a wall followed by splashing, which occurs at high droplet impact velocities. Two types of splashing are distinguished: prompt splashing and delayed splashing [60]. The former is associated with secondary droplet ejection from the crown while it is still growing. With delayed splashing, secondary droplets eject after the crown reaches its maximum height. The critical conditions required to initiate splashing into secondary droplets can be determined using the correlation $K = We \cdot Oh^{-0.4}$. Liang and Mudawar [60] outlined the most promising avenues for further research of droplet impact on a solid surface. In particular, it is research into the heat transfer between a solid wall covered with a liquid film and a falling droplet or a group thereof. These processes should be studied with due consideration of the liquid impact mechanics and the heat transfer coefficient associated with significant heating of a surface, interfacial evaporation, or interfacial condensation. In this context, of special interest are the findings that account for the impact of the wall temperature on the behavior of droplets impinging on it [56–63]. For instance, Šikalo et al. [62] described the heat exchange mechanisms as a result of liquid droplet impact on a heated wall. They explored the influence of droplet velocities, viscosity of liquid (water, glycerol, isopropyl alcohol), surface roughness (smooth and rough glass, wax, polyvinyl chloride), and droplet–wall impact angle. It was experimentally established [62] that an increase in droplet impact velocities on a solid surface increases the spreading rate of the thin liquid layer over the surface provided that the liquid film is boiling. This leads to a reduction in the size of secondary fragments (droplets). It is shown [62] that an increase in the liquid viscosity leads to a significant increase in the size of secondary droplets, and a decrease in the surface roughness reduces the size of the resulting fragments by more than 15%. In addition, the surface roughness is shown to affect the maximum droplet spread diameter. A reduction in the droplet/substrate impact angle from 45° to 15° leads to a significant decrease in the size of secondary droplets. The analysis of research findings [62] indicates that the collision outcome cannot be determined by the Weber number alone. The droplet behavior on a surface is largely determined by the characteristics of liquid. An isopropyl alcohol droplet broke into fragments on a smooth glass surface at the Weber numbers of around 300, whereas the impact of a water droplet on the same surface at the Weber numbers of approximately 1080 did not lead to droplet disruption.

Demidovich et al. [63] arrived at similar conclusions. They determined the main atomization characteristics of liquid droplets impinging on a solid surface with varying roughness, thermophysical characteristics, hydrophilic and hydrophobic behavior, temperature of the wall, impact angle, etc. The main objective of the research was to consider a set of the above factors for analyzing the conditions, under which a fine mist is formed with the necessary characteristics of secondary droplets. As in many other studies, Demidovich et al. [63] used an indicator characterizing the liquid droplet area ratio after and before collision (S_1/S_0) as the atomization intensity indicator. In particular, the droplet size distribution and S_1/S_0 were shown to change depending on the material of the collision surface. The use of metal substrates increases the area ratio to reach $S_1/S_0 \approx 3.8$. The use of surfaces with different roughness classes also led to changes in the area ratio. The maximum value equaled 6.55 for roughness class 3 (average roughness 20; 16; 10 μm ; average peak-to-valley roughness 80; 63; 50; 40 μm). At impact angles of $60\text{--}90^\circ$, the area ratio S_1/S_0 is at its maximum.

It was established that the collision process depends heavily on the wettability of the solid wall in addition to its roughness and thermophysical properties of its material. The impact of the surface material roughness and wettability on its interaction with liquid droplets was studied by Clavijo et al. [64]. The diameter of droplets was 1.9 ± 0.03 mm. The surface roughness was within the range of $0.025\text{--}6.3$ μm . An increase in these parameters was found to provide the intense disruption of droplets impinging on a solid surface. However, the droplet only breaks up if the surfaces are hydrophilic or superhydrophilic (Figure 6). Upon collision with a hydrophobic surface, a droplet deforms and bounces. Clavijo et al. [64] studied the hydrodynamics of water droplet impingement on superheated

solid surfaces (125 °C to 415 °C) in a wide wettability range: superhydrophilic, hydrophilic, hydrophobic, and superhydrophobic. They plotted hydrodynamic characteristics of a droplet as functions of the Reynolds number, Weber number, and surface properties (Figure 7).

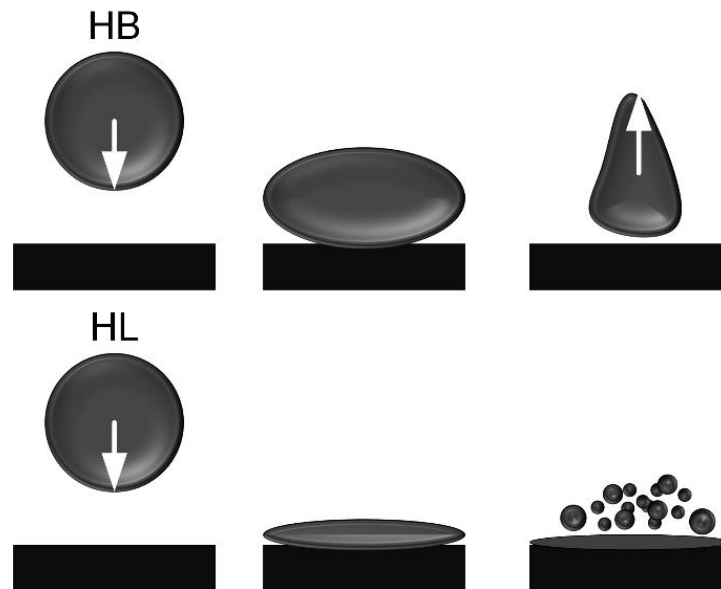


Figure 6. Droplet impingement on a surface: HB stands for hydrophobic surface; HL is hydrophilic surface.

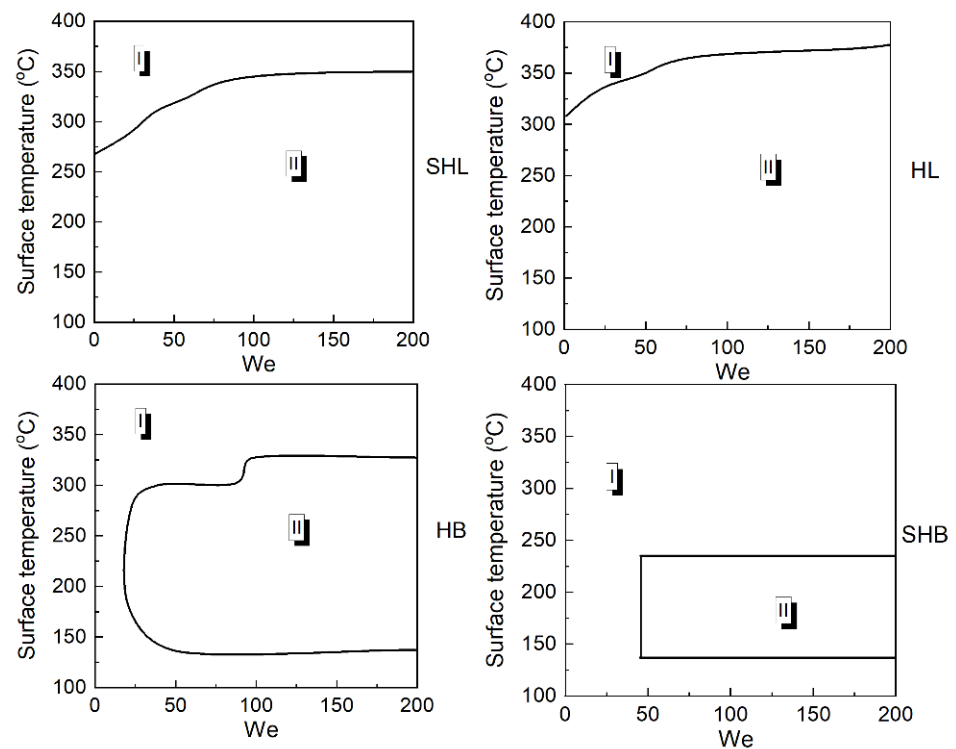


Figure 7. Wall impact regime map plotted using the data from [64]. I—secondary fragments are not formed; II—secondary droplets are formed. HL is hydrophilic surface; SHB denotes superhydrophobic surface; HB stands for hydrophobic surface.

Clavijo et al. [64] found that the maximum number of secondary droplets are formed in a certain average temperature range. Similar conclusions were made from analyzing the experimental data [63] showing that the greatest number of secondary fragments are formed by the impingement on a heated substrate. A limited temperature range was identified (50–100 °C), in which the maximum atomization of impinging droplets occurs. The result correlates well with the findings of previous research [64,65], which also recorded an increase in the number of secondary droplets when the solid surface was heated to certain (critical) temperatures (150–300 °C). Further heating of the wall led to a dramatic decrease in the number of resulting secondary fragments [64,65]. This effect [64,65] is caused by a liquid layer formed on the impingement surface that subsequent droplets interact (merge) with. Demidovich et al. [63] supplemented the conclusions drawn in Refs. [64,65] by a set of hypotheses. In particular, they established that a vapor–gas buffer layer is formed between the droplet and the substrate when the wall temperature exceeds 100 °C. This reduces the intensity of heat transfer from the substrate to the liquid and, hence, the intensity of its heating. In addition, heating to 100 °C leads to water boiling. This boiling causes the micro-explosion of droplets with subsequent atomization (splashing).

The patterns observed in Refs. [66–69] build on the previous research [61–65]. In particular, Sen et al. [67] experimentally studied the impact of alternative jet fuel on a surface heated to 25 to 350 °C. They observed rather intense disruption (splashing) of the fuel film with the formation of a group of secondary droplets upon impact on a substrate heated to the temperatures T_s over 210 °C (Figure 8). When a surface is heated to 280 °C, a crown is formed, and the intensity of its disruption does not differ much from droplet disruption on a substrate at 320 to 350 °C (Figure 8).

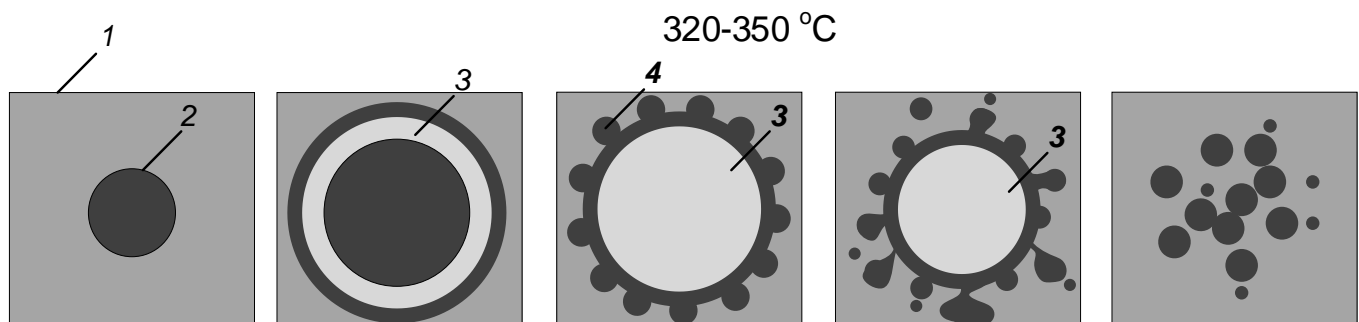


Figure 8. Wall impact regime map (top view): 1—substrate; 2—droplet; 3—liquid film; 4—crown formation.

At substrate temperatures of 150–210 °C and Weber numbers $We = 886$, the number of secondary droplets is found to be much greater than at $We = 166$. The results obtained by Sen et al. [67] are in an acceptable agreement with the patterns established by Fujimoto et al. [68], where the intense disruption of droplets impinging on a substrate at 2.07–2.1 m/s was observed at surface temperatures of about 200 °C. When droplets hit a surface heated to over 300 °C, the liquid assumed a ring-like shape, then coalesced and rebounded off the surface.

Interesting patterns in the successive impingement of a group of droplets on a solid metal surface were observed by Fujimoto et al. [66]. The wall temperature was varied from 25 °C to 500 °C. The successive generation of single droplets (0.39–0.65 mm in size, with a velocity of 2–5 m/s) led to the formation of a liquid layer on a solid surface. As a result, each subsequent droplet interacted with a liquid layer of varying thickness. As a result of such interaction, the so-called liquid crown is formed: When a droplet hits a liquid film, the film swells due to the high pressure at the point of impact. Heating the surface to 300 °C leads to a significant deformation of the first impinging droplet (an oblong liquid crown is formed) with its further breakup into a large number of small-size secondary droplets. When a droplet impinged on a surface heated to 500 °C, no secondary droplets

were formed. Instead, a thin vapor film emerged between the droplet and the surface, which rapidly spread and evaporated.

The research findings [61–65] indicate that it is not feasible to increase the wall temperature above a certain average temperature range in which the secondary droplets are formed most actively. Such data pave the way for reducing the energy cost of wall heating in technological equipment aimed at improving the efficiency of fine mist. It is sensible to single out new methods and approaches to studying the interaction of liquid droplets with solid surfaces [71–75]. The approach used in Refs. [71–75] involved the restitution coefficient (ratio of bounce velocity to initial velocity of a droplet) characterizing the energy dissipation during impact. It was shown that an increase in the thickness and viscosity of the liquid film on a solid surface reduces this coefficient. If the droplet impingement velocity is constant, the restitution coefficient does not depend on the droplet impact angle. Wang et al. [70] studied the rupture of liquid film in vapor–liquid separators using Planar Laser Induced Fluorescence (PLIF). The Reynolds numbers ranged from 1800 to 4200 in the experiments. As part of the experimental research, the authors established the specific height of the liquid film destruction and the droplet size distribution.

Quite interesting results were obtained in the field of theoretical research into liquid droplet interaction with solid walls. In particular, Senda et al. [71] developed a model simulating the formation of a fuel film when a diesel spray impinged on a wall. Importantly, the film broke up to form of an array of interacting droplets. Roisman [72] presented a theoretical description of an unsteady laminar viscous flow in a spreading film of a Newtonian fluid. Such flow is generated by a drop impact onto a solid surface with high Weber and Reynolds numbers. A numerical solution for the viscous flow in the spreading droplet is obtained which satisfies the Navier–Stokes equation. The research findings [72] established the maximum spreading diameter of a droplet colliding with a solid surface as a key droplet/wall interaction parameter. This parameter largely depends on the Weber and Reynolds numbers, as well as on the substrate wettability. However, if the We and Re are high, the effect of wettability is negligible. Several modes of spreading were distinguished [72]: droplet impact on a wall with low Weber and Reynolds numbers ($We < 10$, $Re < 100$); a collision when $We > 10$ and $Re > 100$ (in this mode, the droplet shape can be represented as a radially spreading lamella when the flow in the lamella is inertia dominated); droplet impact leading to the maximum spreading diameter determined mainly by the viscous effects. The above research findings hold great potential for industrial application, especially since materials are being developed for protection against pollution, icing, and corrosion [73].

5. Droplet Collision with a Gas Jet

The discharge of a gas jet to break up droplets into a large number of fine fragments is used in many technical applications (in particular, in fuel combustion [74]) to intensify the evaporation processes [75–80]. At high liquid droplet velocities and gas densities, the aerodynamic asymmetry of a jet could dramatically promote liquid breakup [81]. Aerodynamic forces acting on a droplet deform it significantly and, if such forces have a high magnitude, they break up a droplet into a large number of small fragments [81]. Research in this field follows two lines: identifying critical (transient) conditions between regimes [75–80] and determining the integral characteristics of the atomization processes [82].

Fundamental research (both theoretical and experimental) into the deformation of droplets exposed to an air flow was generalized and presented in Refs. [74,76,77]. As a result, two main parameters were identified that affect the droplet disruption behavior: the Weber number and the Reynolds number. The breakup process occurs in three main stages: droplet deformation, formation of a rim, and its further expansion and fragmentation. Experimental and theoretical research findings [7,76,78–80] accumulated over the last 50–70 years made it possible to outline the main breakup regimes of droplets exposed to an air flow [78]. However, to describe the breakup dynamics, the regimes are further classified into the following ones [76]: vibrational breakup ($We = 10–15$), bag breakup

($We = 15\text{--}20$), bag-and-stamen breakup ($We = 50\text{--}70$), stripping breakup (continuous shift) ($We = 800\text{--}1000$), and explosive or catastrophic breakup ($We > 5000$).

The disruption of droplets exposed to aerodynamic forces is often analyzed by directing a high-speed air jet at suspended droplets. In particular, Jackiw and Ashgriz [83] obtained the images of droplets and their disruption process with a high temporal and spatial resolution to show the manner of droplet breakup into small fragments, as well as their number and size. They hypothesize that droplet disruption is governed by its internal stream. They also presented a calculated prediction of the number and size of secondary droplets. Interesting results were obtained by Chou and Faeth [82], who experimentally studied the temporal indicators of droplet disruption by an air flow at standard temperature and pressure. The Weber numbers were varied in the range of 13–20, the Ohnesorge numbers equaled 0.0043–0.0427, and the Reynolds numbers ranged from 1550 to 2150. The liquid ring formed from the original droplet contained 56% of the initial droplet volume (mass) and when it broke up, it formed droplets with a 30% lower average diameter as compared to the original droplet size. The liquid bag formed under aerodynamic forces was a monolith containing about 44% of the initial droplet volume (mass). It broke up into virtually monodisperse droplets with an average diameter of about 4% of the original droplet diameter. The duration of the initial droplet breakup was about 3.2 to 3.5 s. It was established [82] that such disruption could provide an almost monodisperse droplet size distribution.

Flock et al. [76] presented the results of their experimental research into the deformation behavior of single ethyl alcohol droplets injected into a continuous air jet. The experiments were conducted for the conditions in which the regimes of bag breakup and stripping breakup occurred to find the average diameter of the resulting droplets, as well as their trajectories and velocities. No significant impact of droplet evaporation was observed on droplet breakup by an air jet. Experimental results obtained in Ref. [76] are useful for the development of physical models and validation of Eulerian–Lagrangian simulation techniques.

The research findings on the breakup of droplets of Newtonian and viscoelastic fluids in a high-speed air stream ($We = 11,700\text{--}16,900$, $Re = 40,000\text{--}127,600$) were presented by Joseph et al. [84]. When exposed to this stream, water droplets of a millimeter diameter were reduced to mist after 500 μs . The data obtained made it possible to determine the acceleration of viscous droplets required for their intense fragmentation ($10^4\text{--}10^5$ times as high as free-fall acceleration) [84]. The shock wave Mach number is shown to increase significantly with an increase in the liquid viscosity.

Voytkov et al. [85] recorded the transformation and breakup characteristics of droplets of typical fire suppressants (water and water-based slurries and emulsions) exposed to aerodynamic forces (the air flow velocity ranged from 0.5 to 50 m/s). Three regimes were identified: surface transformation without breakup, bag formation followed by its destruction, and breakup into a cloud of small droplets (catastrophic breakup). Critical We and Re numbers were determined for complete (catastrophic) breakup. It was shown that, in order to increase the free surface area by more than 10 times, the air flow should be supplied at a velocity of over 50 m/s and the liquid compositions should be highly heterogeneous. The results obtained in Ref. [85] can be used to develop extinguishing media, heat exchange chambers, thermal water treatment technologies, as well as environmentally friendly fuel technologies due to water and water vapor capturing the hazardous anthropogenic emissions.

The research findings by Soni et al. [86] deserve special attention. They experimentally investigated the deformation and breakup of droplets interacting with an oblique continuous air stream (the nozzle orientation was varied from 0 to 60°). In addition to the air stream impact angle, they studied the impact of droplet size and liquid properties (surface tension and viscosity) on breakup regimes. The critical Weber numbers for droplet breakup were obtained as a function of the angle of inclination of the air stream and the

Ohnesorge number. The departure from the cross-flow arrangement led to a significant decrease in the critical Weber numbers for the bag breakup.

An increase in the obliquity angle of the air flow prolongs the droplet breakup time. This effect was attributed to the decelerated curvilinear motion of a droplet [86]. In addition, an increased viscosity of the liquid (increased Ohnesorge numbers) requires higher We for the droplet to undergo the bag breakup. Similar conclusions are formulated in Ref. [84].

The above research findings indicate that droplet exposure to an oncoming air flow significantly increases the probability of droplet fragmentation. However, the use of this technique causes a significant excess of gas (air) in the combustion chamber [74], increasing both the economic expenses and the concentration of nitrogen dioxide. It is also known that at high droplet flow velocities [78], droplets break up due to the domination of friction and drag forces over the surface tension. However, this droplet atomization technique is economically unfeasible because the existing heat exchangers and combustion chambers need to be pressurized, which increases their cost and wear.

6. Micro-Explosive Breakup of Droplets

The micro-explosive breakup of droplets of liquids, slurries, and emulsions enables a several-fold increase in their evaporation surface area (Figure 9). This effect reduces the energy and time costs of fuel heating, evaporation, and ignition. It also decreases the anthropogenic emissions and provides more complete fuel combustion. The present-day systems of thermal and flame water treatment, as well as other principally different systems, unfortunately cannot provide high performance [87,88]. This is because the liquid to be treated needs to be fed to the thermal treatment chamber repeatedly. Impurities cannot evaporate or burn out completely during just one cycle in the heating chamber. Therefore, the energy consumption of these systems increases and so does the duration of the corresponding processes. In thermal liquid treatment and fuel technologies, this problem can be solved by droplet breakup into smaller fragments with a typical size of several dozens to several hundreds of microns. However, as the experiments [89] show, droplets this small moving at low velocities may stick to the walls of the combustion chamber walls or they may be entrained by high-velocity hot flue gases or incoming air flow and blown away from the thermal treatment chamber. Thus, preliminary droplet breakup before supplying them to heating chambers may result in technological limitations and complications. In this case, it is practical to start droplet disintegration in thermal treatment or combustion chambers in the process of heating. Researchers from all over the world endeavor to develop the corresponding technologies. The most effective ones in terms of stability as well as the required energy and time t involve explosive droplet boiling and breakup to form a fuel spray.

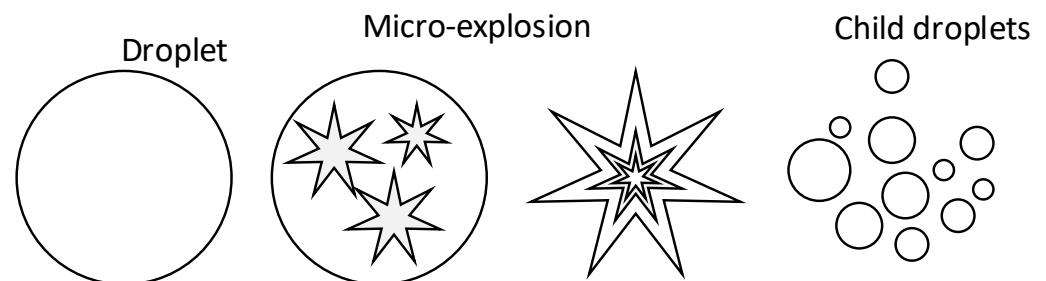


Figure 9. Scheme of micro-explosive breakup.

Researchers [90–92] were among the first to pay attention to splashing in the puffing regime and explosive breakup of boiling fuel droplets. According to their data, these processes are largely governed by molecular interactions, as well as the amount and concentrations of vapor bubbles emerging in droplets. Refs. [90,91] establish that CO_2 -rich water emulsion droplets require less superheating and shorter heating time for boiling

and breakup. These data explain the reasons why water emulsion droplets heat up and boil after a shorter time. In Refs. [90,91], the explosive breakup of emulsion droplets required high concentrations of petroleum products and high temperatures. The role of CO₂ under such conditions is significant [90,91]. Therefore, it took less heating time for water emulsion droplets to boil and break up into a large aerosol cloud with a distinct CO₂ smell. Using a mathematical model based on the experimental data from Refs. [90,91], one can predict how CO₂ will influence the heating and boiling of water emulsion droplets. Experimental research by Won et al. [49] showed that water-in-oil emulsions show higher combustion efficiency associated with lower emissions as compared to conventional fuels. Such improvements, according to Won et al. [49], become possible due to micro-explosions. The emulsion containing 0.2% of mixed surfactant was found optimal [49]. Ref. [49] shows that the temperature of the onset of micro-explosion increases with an increase in the fuel injection pressure.

Experimental studies presented in Refs. [92,93] distinguished the following stages of heterogeneous droplet vaporization: evaporation from its free surface, bubble boiling at the internal interfaces, growth of bubbles and droplet enlargement with a decrease in the liquid film thickness around the inclusion, and explosive breakup (separation of a group of fragments with vapor and air bubbles in them). The authors established that adding <0.05-mm nontransparent carbonaceous inclusions (with a mass fraction under 2%) to water droplets contributes to a 40–50% reduction in droplet lifetimes compared with droplets containing only one nontransparent solid inclusion in the case of evaporation from an external surface. They also established the impact of a vapor layer forming around droplets and serving as an extra thermal insulation due to low thermal conductivity on the intensity of droplet evaporation. When a water droplet with a solid inclusion is heated in the air at over 1000 K, the evaporation surface area may increase by 3–15 times relative to the original droplet surface area due to intense liquid vaporization with an explosive breakup into small droplets [92,93].

Refs. [92,93] established the integral characteristics of boiling, surface transformation, and superheating for droplets of water and water-based slurries when radiative heat flux from the surrounding gas dominates the convective one. They identified the necessary and sufficient conditions for the explosive breakup of boiling water slurry droplets with carbonaceous and soil additives, as well as for slow evaporation with the droplet retaining its integrity. The first simplified models were developed simulating the heat and mass transfer controlling for the explosive breakup of droplets heated in a high-temperature gas [92,93].

Studies by Meng et al. [94] showed that the micro-explosion characteristics depend heavily on the flow of the heating medium: the higher the heated gas flow rate is, the shorter the micro-explosion delay becomes and the smaller the secondary droplets are. Refs. [95–97] experimentally showed how the micro-explosion affects the ignition and combustion characteristics of multicomponent fuels. It was established that micro-explosion and changing the fuel chemical composition by adding oxygen-containing compounds [98] accelerates combustion and decreases soot production [95–97] due to more intense mixing of fuel and surrounding oxidizing gases. Moreover, the component ratio was found to have a significant influence on fuel spraying and ignition [95–97]. The experimental data obtained by Wang et al. [97] show that the occurrence of micro-explosion also depends on the regimes, in which two-liquid droplets are formed during component interaction. For example, for collision-produced droplets, a bubble is more likely to emerge in a droplet if the impact velocity is higher and the collision is not head-on, which, in turn, increases the chance of micro-explosion. Wang et al. [97] also established that a micro-explosion significantly accelerates the combustion.

The mechanisms of micro-explosive breakup of multicomponent droplets were investigated with several hypotheses formulated [99,100] about the physics of such processes. In a series of complex experiments, Wang et al. [99] showed that micro-explosion occurs when one or two large bubbles emerge near the droplet center, which contributes to more

effective fragmentation. The bubble generation is directly influenced by the difference in the component volatilities. For a bubble to emerge in a droplet, it must be heated to the boiling temperature of the least volatile component [99]. Research by Li et al. [100] showed that bubble nucleation in a droplet with its subsequent breakup depends on the degree of superheating—there must be a critical change in temperature. Li et al. established [100] that breakup occurs due to bubbles expanding inside a droplet and its surface tension decreasing because of superheating. Another breakup mechanism is the high velocities of convective flows at the interface between two components. They trigger the disruption of the inter-component interface and then the full breakup of the droplet [100]. For droplet disruption modeling, it is linked to critical Weber and Reynolds numbers. At higher Weber numbers, the liquid structure tends to break up into small fragments, and turbulent dissipation is generally minimized. For low Weber numbers, critical Reynolds numbers are determined corresponding to the onset of droplet disruption.

One of the first and quite simple micro-explosion models for typical heterogeneous liquid droplets was presented by Law in 1978 [101]. When heated, the least volatile component concentrates in the center of a droplet. It may reach the temperatures sufficient for bubble nucleation, which triggers droplet breakup [101]. Over the recent years, studies in this field have been undertaken all over the world. In particular, Sazhin et al. [102] presented a simplified micro-explosive breakup model based on the solution of the heat equation. The water boiling temperature reached by the droplet surface was regarded as the threshold condition for the micro-explosive breakup. Sazhin et al. introduced a series of restrictions to significantly simplify the calculations, which, however, reduced the agreement between the simulated and experimental characteristics of micro-explosive fragmentation [102]. The agreement was only good enough at high temperatures and pressures in the heating chamber and with extremely small droplet size. The corresponding conclusions were formulated by Sazhin et al. [102] after comparing the data obtained from simulations and a series of experiments. They present their model [102] as a first approximation, sufficient for predictive evaluations of the micro-explosive breakup characteristics of emulsified fuels.

According to the preliminary analysis [103,104], the duration of two-component droplet heating and breakup as well as the size and number of resulting droplets largely depend on the concentration of components and the heat flux supplied to the droplet surface. With emulsion droplets, it is necessary to add such important factors as [103,104]: size of discontinuous phase droplets (water droplets in a combustible liquid, for instance, diesel), size of emulsion droplets, water content in the emulsion, as well as the concentration and type of stabilizer. To investigate the impact of the most important factors from the list above, experiments were carried out [103,104] with varying temperature in the muffle furnace, air flow temperature and velocity, as well as the concentration and type of the liquid combustible component. It was shown [103,104] that droplet lifetimes before swelling and micro-explosion decrease nonlinearly with an increase in the ambient temperature (Figure 10). This was linked to the non-linear (exponential) dependence of the evaporation rates of combustible and non-combustible liquid components on temperature [103,104]. Here, the more large-scale the changes in these velocities with the rising temperature and the lower the boiling, ignition, and flash temperatures of combustible components, the more significant the changes in the heating times until explosive breakup (τ) (in particular, Figure 10 shows a 44% difference between the parameter τ for the emulsion containing 5% of petroleum differs and that of the emulsion containing 5% of transformer oil). In some cases, as noted in Refs. [103,104], droplet puffing was difficult to record due to considerable surface transformations of droplets moving towards the channel with heated air as well as due to droplets breaking away from the holder. Therefore, the curves are not obtained for all the compositions in the temperature range of 250 to 550 °C.

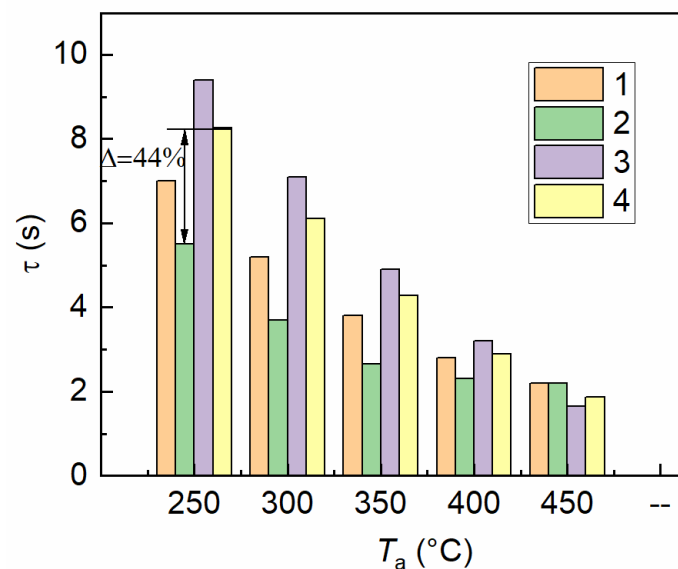


Figure 10. Comparison of droplet (15 μ L) heating times for various compositions to explosive breakup versus gas temperature (using the results [103]): 1—emulsion (97% water, 3% petroleum); 2—emulsion (95% water, 5% petroleum); 3—emulsion (97% water, 3% oil); 4—emulsion (95% water, 5% oil).

The breakup times of two-liquid droplets in the muffle furnace experiments are found to be several times longer than in the experiments with incoming heated air (Figure 10) at identical temperatures. This happens because the convective heat flux from the air flow to the droplet surface is several times greater than the radiative heat flux from the muffle furnace walls at such mild temperatures [104]. In particular, the radiative heat flux starts dominating the convective one at above 800 °C [104].

The global scientific community is still in search of methods to control the explosive breakup (disruption) of droplets of combustible liquids, fuels, as well as two immiscible fluids, emulsions, solutions, or slurries. Mathematical and physical models should be developed to reliably predict droplet breakup outcomes after local superheating and boiling, as well as regimes of these processes, differences between various mixing schemes, etc. This is only possible with a reliable experimental database of characteristics and conditions for these effects.

7. Combined Atomization Schemes

When using the atomization schemes described above, it makes sense to combine them to intensify the generation of a droplet flow with the required particle size distribution, as well as to reduce the economic and time costs. Very few studies have been conducted so far on the integral characteristics of droplet atomization using well-known secondary atomization schemes (among them are Refs. [97,105,106]). Such characteristics should be compared by determining the mean and maximum sizes of secondary fragments and their total surface area. The choice of secondary atomization methods to be combined is relevant in many applications. Several secondary droplet atomization schemes used one after another will significantly increase the free surface area of a liquid. For instance, the use of several secondary atomization methods plays an important role in liquid purification technologies.

From the analysis of the literature quoted in Sections 4 and 6, we can make a reasonable conclusion that the most efficient droplet atomization is provided by droplet interaction with a solid wall and by micro-explosive breakup. With this in mind, it would be reasonable to reduce the cost of these processes. To avoid the use of extra heaters for the surfaces that droplets break up on, it is sensible to position high-power heating elements, furnaces, and chambers next to solid heating surfaces. The heat flux from furnaces and heating chambers, in which micro-explosive breakup occurs, can be supplied to the surfaces involved in the

intense atomization of liquid fragments. The research findings in this field are given in Refs. [97,105,106]. Wang et al. [97] investigated droplet atomization arranged in two stages. At the first stage, binary droplet collisions took place leading to droplet coalescence (the original droplet size was varied from 0.1 to 0.4 mm). The resulting liquid droplets fell through a vertical channel connected to a high-temperature combustion chamber to provide droplet micro-explosion (second atomization stage). Micro-explosive breakup was only observed for coalesced droplets. The authors hypothesized that this process was initiated by air bubbles entrained by droplets during their interaction. The potential importance of bubble nucleation in colliding droplets on spray atomization was emphasized. The probability of bubble nucleation inside droplets was shown to increase with an increase in the impact velocities and off-centeredness. The research findings [97] indicate that the simultaneous use of several secondary atomization methods can only be effective if the spraying parameters were well selected at the previous stages, including the sizes and velocities of initial droplets, component composition of the liquid, impact angles, etc.

Kuznetsov et al. [105] determined the conditions for the use of various secondary atomization techniques to produce a mist of minimum-sized droplets with a relatively low electric power consumption. They used an experimental setup that provided droplet collisions with each other followed by their exposure to an air flow. At the last stage, droplets collided with a solid wall. Kuznetsov et al. [105] combined several secondary atomization schemes: droplet–droplet collisions, exposure to a gas flow, collisions with a heated wall, and micro-explosion. This combination was shown to provide a severalfold increase in the free surface area of the liquid as compared to using one of the atomization mechanisms described above (Figure 11). A significant growth of this indicator occurs at the third atomization stage—the disruption of earlier atomized droplets on a heated solid wall. The least active generation of secondary droplets occurs due to the combination of three droplet atomization schemes: droplet–droplet collision, droplet breakup on a solid surface, and micro-explosive breakup. However, this scheme can be made more effective by using a heated surface at the second stage. Based on the generalized data given in Figure 11, the following conclusion was made [105]: When several secondary atomization schemes are used, the greatest contribution comes from the impact of droplets on a heated solid wall after their preliminary atomization by colliding with each other and exposure to the incoming air flow. Intense droplet fragmentation is also observed when the micro-explosive breakup is used at the last step of combined atomization.

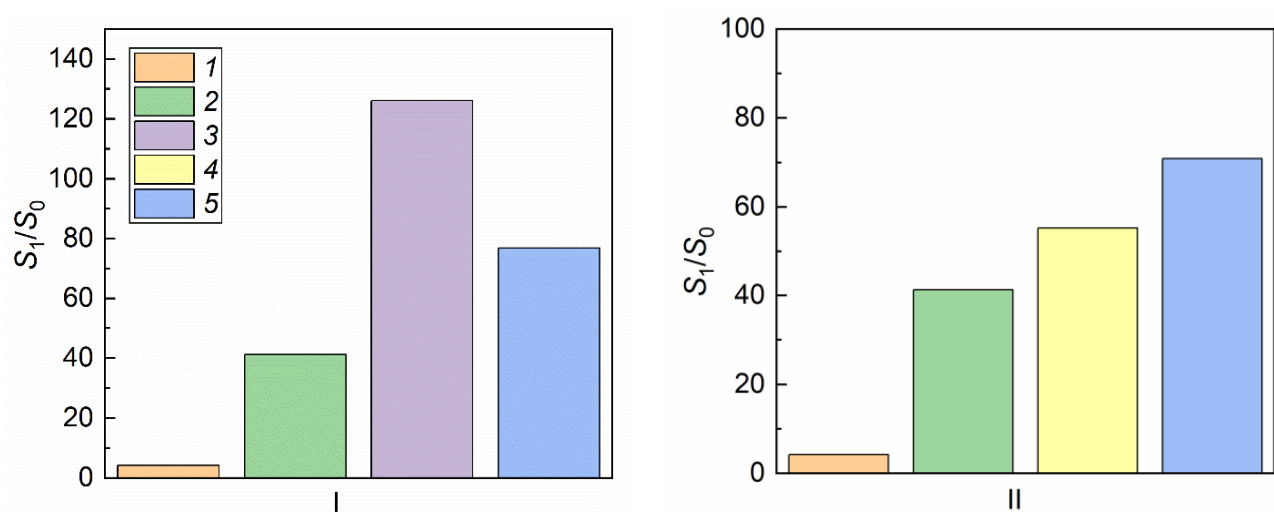


Figure 11. Maximum surface area ratio of an emulsion containing 90 vol% of diesel and 10 vol% of water for combining most effective schemes (I–II), described in [105]: 1—droplet–droplet collisions; 2—exposure to air flow; 3—collision with a heated solid surface; 4—collision with a cold wall; 5—micro-explosive breakup.

Kuznetsov et al. [105] presented the curves for the ratio of the average post-collision fragment size to the original droplet size by combining several atomization schemes (droplet–droplet collision, atomization by a gas jet, droplet collision with a surface, and micro-explosive breakup). The results obtained by Kuznetsov et al. [105] were compared with those obtained by Davanlou et al. [106] also using several secondary atomization schemes. When comparing the data from Refs. [97,105], 30–40% deviations were found, which Kuznetsov et al. [105] linked to differences in the sequence of atomization stages. Binary droplet collisions took place at the first stage [97] and micro-explosive breakup followed at the second stage. However, the combination of atomization schemes in this sequence prolonged the droplet disruption, which is a crucial parameter for the practical application of the technology in industrial combustion chambers [105]. It was experimentally established [105] that intense atomization of both homogeneous and heterogeneous liquids can be provided by combining four secondary atomization schemes. Recommendations were formulated on the simultaneous application of such schemes that can ensure the maximum intensity of droplet spray generation. The first atomization stage should involve droplet collisions followed by an air jet impact at the second stage. Then it is advisable to provide droplet atomization through collisions with a heated wall followed by the micro-explosive breakup of droplets heated in special-purpose chambers and furnaces [105]. This combination will increase the free surface area of emulsions by 250 times. For slurry droplets, the S_1/S_0 indicator is somewhat lower, namely, 170 to 190. However, such high ratios cannot be achieved for water because it is impossible to provide micro-explosive breakup of homogeneous water droplets without solid or liquid additives.

The data obtained in Refs. [97,105,106] are of great practical importance because they make it possible to select secondary atomization schemes to be combined depending on the size of secondary droplets required by a specific technology and their component composition. In particular, the heat of the high-temperature gases coming from furnaces can be used in liquid treatment to heat the walls of evaporators and the air therein. This provides conditions for droplet disruption on a heated wall and for their micro-explosive breakup. The research findings [105] have shown that 400–500 °C is a sufficient temperature for the wall surface heating to provide intense droplet atomization. According to Kuznetsov et al. [105], liquid treatment after the injection of the initial spray will take several seconds in this temperature range at each atomization stage.

8. Conclusions

In this analysis, we have summarized the experimental and theoretical research findings on liquid droplet coalescence, disruption, and fragmentation in multiphase and multicomponent gas-vapor-droplet media. These processes can be studied using phenomenological and applied approaches, and both have been considered in this paper. The analysis of the known research findings has shown that scientific foundations have been laid for the modern theory of liquid droplet interactions in a gaseous medium. We have presented the main elements of these scientific foundations. The generalized curves, tables, and approximations can be used to predict the conditions and characteristics of liquid droplet coalescence, disruption, and fragmentation in multiphase and multicomponent gas-vapor-droplet media. The systematized experimental and theoretical research findings expand the contemporary notions of liquid droplet interactions in a gas. At this point, it is safe to conclude that the most promising technologies of secondary atomization of liquid droplets can be introduced using a combination of several techniques: droplet–droplet collisions, droplet collisions with a solid wall, exposure to a gas jet, and micro-explosive breakup.

Author Contributions: P.S. contributed to the analysis of the results and preparation of the text of the paper; S.K. analyzed the results of researchers in the chosen scientific direction and wrote the article. Both authors have read and agreed to the published version of the manuscript.

Funding: Research was supported by the Russian Science Foundation (project 18-71-10002- π , <https://rscf.ru/en/project/21-71-03001/>).

Conflicts of Interest: The authors declare no conflict of interest.

Nomenclature

Greek letters

α_d	impact angle, $^\circ$.
Δ	droplet size ratio.
τ	heating time until explosive breakup, s.

Latin letters

b	linear approach parameter, mm.
B	dimensionless linear interaction parameter.
D_{32}	Sauter diameter, μm .
F_T	injection in percentage terms, %.
h^*	non-dimensional film thickness.
L_{nd}	non-dimensional length scale of wall roughness.
N	number of child droplets.
Oh	Ohnesorge number.
P	injection pressure, bar.
R_{d1}, R_{d2}	radius of the first and second droplet, respectively, mm.
R_{nd}	the non-dimensional wall roughness parameter.
r_d	radius of child droplets, mm.
Re	Reynolds number.
S_0	surface area of two initial colliding droplets, mm^2 .
S_1	area of newly formed fragments after the collision of two initial droplets, mm^2
S_1/S_0	ratio of areas before and after collision.
T_a	gas temperature, $^\circ\text{C}$.
T_S	substrate temperatures, $^\circ\text{C}$.
T_g	temperature of a hot air flow, $^\circ\text{C}$.
t	time of explosive droplet boiling and breakup to form a fuel spray, s.
U_{d1}, U_{d2}	velocities of initial droplets, m/s.
U_{rel}	resultant droplet velocity, m/s.
We	Weber number.

References

- Daho, T.; Vaitilingom, G.; Sanogo, O. Optimization of the combustion of blends of domestic fuel oil and cottonseed oil in a non-modified domestic boiler. *Fuel* **2009**, *88*, 1261–1268. [[CrossRef](#)]
- Finotello, G.; Padding, J.T.; Buist, K.A.; Schijve, A.; Jongsma, A.; Innings, F.; Kuipers, J.A.M. Numerical investigation of droplet-droplet collisions in a water and milk spray with coupled heat and mass transfer. *Dry. Technol.* **2020**, *38*, 1597–1619. [[CrossRef](#)]
- Zhang, H.; Li, Y.; Li, J.; Liu, Q. Study on separation abilities of moisture separators based on droplet collision models. *Nucl. Eng. Des.* **2017**, *325*, 135–148. [[CrossRef](#)]
- Planchette, C.; Lorceau, E.; Brenn, G. Liquid encapsulation by binary collisions of immiscible liquid drops. *Colloids Surfaces A Physicochem. Eng. Asp.* **2010**, *365*, 89–94. [[CrossRef](#)]
- Orme, M. Experiments on droplet collisions, bounce, coalescence and disruption. *Prog. Energy Combust. Sci.* **1997**, *23*, 65–79. [[CrossRef](#)]
- Finotello, G.; De, S.; Vrouwenvelder, J.C.R.; Padding, J.T.; Buist, K.A.; Jongsma, A.; Innings, F.; Kuipers, J.A.M. Experimental investigation of non-Newtonian droplet collisions: The role of extensional viscosity. *Exp. Fluids* **2018**, *59*, 113. [[CrossRef](#)]
- Krishnan, K.G.; Loth, E. Effects of gas and droplet characteristics on drop-drop collision outcome regimes. *Int. J. Multiph. Flow* **2015**, *77*, 171–186. [[CrossRef](#)]
- Arkhipov, V.A.; Ratanov, G.S.; Trofimov, V.F. Experimental investigation of the interaction of colliding droplets. *J. Appl. Mech. Tech. Phys.* **1978**, *19*, 201–204. [[CrossRef](#)]
- Ko, G.H.; Ryou, H.S. Modeling of droplet collision-induced breakup process. *Int. J. Multiph. Flow* **2005**, *31*, 723–738. [[CrossRef](#)]
- Yarin, A.L.; Roisman, I.V.; Tropea, C. *Collision Phenomena in Liquids and Solids*. Cambridge University Press: Cambridge, UK, 2017.
- Brenn, G.; Valkovska, D.; Danov, K.D. The formation of satellite droplets by unstable binary drop collisions. *Phys. Fluids* **2001**, *13*, 2463–2477. [[CrossRef](#)]

12. Tkachenko, P.P.; Shlegel, N.E.; Volkov, R.S.; Strizhak, P.A. Experimental study of miscibility of liquids in binary droplet collisions. *Chem. Eng. Res. Des.* **2021**, *168*, 1–12. [[CrossRef](#)]
13. Estrade, J.-P.; Carentz, H.; Lavergne, G.; Biscos, Y. Experimental investigation of dynamic binary collision of ethanol droplets – a model for droplet coalescence and bouncing. *Int. J. Heat Fluid Flow* **1999**, *20*, 486–491. [[CrossRef](#)]
14. Yoshino, M.; Sawada, J.; Suzuki, K. Numerical simulation of head-on collision dynamics of binary droplets with various diameter ratios by the two-phase lattice kinetic scheme. *Comput. Fluids* **2018**, *168*, 304–317. [[CrossRef](#)]
15. Hu, C.; Xia, S.; Li, C.; Wu, G. Three-dimensional numerical investigation and modeling of binary alumina droplet collisions. *Int. J. Heat Mass Transf.* **2017**, *113*, 569–588. [[CrossRef](#)]
16. Liu, Z.; Wu, J.; Zhen, H.; Hu, X. Numerical Simulation on Head-On Binary Collision of Gel Propellant Droplets. *Energies* **2013**, *6*, 204–219. [[CrossRef](#)]
17. Saffman, P.G.; Turner, J.S. On the collision of drops in turbulent clouds. *J. Fluid Mech.* **1956**, *1*, 16–30. [[CrossRef](#)]
18. Qian, J.; Law, C.K. Regimes of coalescence and separation in droplet collision. *J. Fluid Mech.* **1997**, *331*, 59–80. [[CrossRef](#)]
19. Kuschel, M.; Sommerfeld, M.; Verfahrenstechnik, M.; Halle-Wittenberg, M.-L.-U. Experimental investigation of droplet collisions with higher viscosity. In Proceedings of the 23rd Annual Conference on Liquid Atomization and Spray Systems, Brno, Czech Republic, 6–9 September 2010.
20. Finotello, G.; Kooiman, R.F.; Padding, J.T.; Buist, K.A.; Jongsma, A.; Innings, F.; Kuipers, J.A.M. The dynamics of milk droplet–droplet collisions. *Exp. Fluids* **2017**, *59*, 17. [[CrossRef](#)]
21. Rozhkov, A.; Prunet-Foch, B.; Vignes-Adler, M. Impact of water drops on small targets. *Phys. Fluids* **2002**, *14*, 3485–3501. [[CrossRef](#)]
22. Pavlenko, I.; Sklabinskyi, V.; Doligalski, M.; Ochowiak, M.; Mrugalski, M.; Liaposhchenko, O.; Skydanenko, M.; Ivanov, V.; Włodarczak, S.; Woziwodzki, S.; et al. The Mathematical Model for the Secondary Breakup of Dropping Liquid. *Energies* **2020**, *13*, 6078.
23. Pavlenko, I.; Liaposhchenko, O.; Sklabinskyi, V.; Storozhenko, V.; Mikhajlovskiy, Y.; Ochowiak, M.; Ivanov, V.; Pitel, J.; Starynskiy, O.; Włodarczak, S.; et al. Identification of the Interfacial Surface in Separation of Two-Phase Multicomponent Systems. *Processes* **2020**, *8*, 306. [[CrossRef](#)]
24. Chen, R.-H.; Wang, W.-C.; Chen, Y.-W. Like-drop collisions of biodiesel and emulsion diesel. *Eur. J. Mech. B Fluids* **2016**, *60*, 62–69. [[CrossRef](#)]
25. Piskunov, M.V.; Shlegel, N.E.; Strizhak, P.A. Effects of target and projectile parameters on collision characteristics of water droplets. *At. Sprays* **2020**, *30*, 171–187. [[CrossRef](#)]
26. Abouelsoud, M.; Li, X.; Peng, L.; Bai, B. Crown behavior during a concentric collision of a falling droplet onto a sessile droplet. *Exp. Fluids* **2018**, *59*, 162. [[CrossRef](#)]
27. Sommerfeld, M.; Kuschel, M. Modelling droplet collision outcomes for different substances and viscosities. *Exp. Fluids* **2016**, *57*, 187. [[CrossRef](#)]
28. Williams, Y.O.; Roas-Escalona, N.; Rodríguez-Lopez, G.; Villa-Torrealba, A.; Toro-Mendoza, J. Modeling droplet coalescence kinetics in microfluidic devices using population balances. *Chem. Eng. Sci.* **2019**, *201*, 475–483. [[CrossRef](#)]
29. Acevedo-Malavé, A.; Loaiza, N. Fluid mechanics calculations in physics of droplets – IV: Head-on and off-center numerical collisions of unequal-size drops. *J. Comput. Multiph. Flows* **2016**, *8*, 148–156. [[CrossRef](#)]
30. Gao, T.-C.; Chen, R.-H.; Pu, J.-Y.; Lin, T.-H. Collision between an ethanol drop and a water drop. *Exp. Fluids* **2005**, *38*, 731–738. [[CrossRef](#)]
31. Focke, C.; Kuschel, M.; Sommerfeld, M.; Bothe, D. Collision between high and low viscosity droplets: Direct Numerical Simulations and experiments. *Int. J. Multiph. Flow* **2013**, *56*, 81–92. [[CrossRef](#)]
32. Chen, R.-H.; Chen, C.-T. Collision between immiscible drops with large surface tension difference: Diesel oil and water. *Exp. Fluids* **2006**, *41*, 453–461. [[CrossRef](#)]
33. Baumgartner, D.; Brenn, G.; Planchette, C. The influence of viscosity on the outcome of collisions between liquid droplets and another immiscible liquid jet. *At. Sprays* **2020**, *30*, 811–823. [[CrossRef](#)]
34. Shlegel, N.E.; Tkachenko, P.P.; Strizhak, P.A. Influence of viscosity, surface and interfacial tensions on the liquid droplet collisions. *Chem. Eng. Sci.* **2020**, *220*, 115639. [[CrossRef](#)]
35. Tkachenko, P.P.; Shlegel, N.E.; Strizhak, P.A. Collisions of water droplets in the high-temperature air. *Int. J. Heat Mass Transf.* **2021**, *170*. [[CrossRef](#)]
36. Kuznetsov, G.V.; Strizhak, P.A. Collisions between Liquid Drops of Various Shapes in a Gas Flow. *Tech. Phys. Lett.* **2019**, *45*, 267–270. [[CrossRef](#)]
37. Tkachenko, P.P.; Shlegel, N.E.; Strizhak, P.A. Interaction between droplets of solutions in a heated gaseous medium. *Powder Technol.* **2021**, *390*, 86–96. [[CrossRef](#)]
38. Strotos, G.; Malgarinos, I.; Nikolopoulos, N.; Gavaises, M. Numerical investigation of aerodynamic droplet breakup in a high temperature gas environment. *Fuel* **2016**, *181*, 450–462. [[CrossRef](#)]
39. Dupuy, P.M.; Lin, Y.; Fernandino, M.; Jakobsen, H.A.; Svendsen, H.F. Modelling of high pressure binary droplet collisions. *Comput. Math. with Appl.* **2011**, *61*, 3564–3576. [[CrossRef](#)]
40. Kuznetsov, G.V.; Piskunov, M.V.; Shlegel, N.E.; Strizhak, P.A. Experimental research of the vapor zone between two coalescing droplets of heated water. *Int. Commun. Heat Mass Transf.* **2021**, *126*, 105410. [[CrossRef](#)]

41. Gac, J.M.; Gradoń, L. Lattice-Boltzmann modeling of collisions between droplets and particles. *Colloids Surfaces A Physicochem. Eng. Asp.* **2014**, *441*, 831–836. [[CrossRef](#)]
42. Pawar, S.K.; Henrikson, F.; Finotello, G.; Padding, J.T.; Deen, N.G.; Jongasma, A.; Innings, F.; Kuipers, J.A.M.H. An experimental study of droplet-particle collisions. *Powder Technol.* **2016**, *300*, 157–163. [[CrossRef](#)]
43. Yang, B.; Chen, S. Simulation of interaction between a freely moving solid particle and a freely moving liquid droplet by lattice Boltzmann method. *Int. J. Heat Mass Transf.* **2018**, *127*, 474–484. [[CrossRef](#)]
44. Malgarinos, I.; Nikolopoulos, N.; Gavaises, M. Numerical investigation of heavy fuel droplet-particle collisions in the injection zone of a Fluid Catalytic Cracking reactor, Part I: Numerical model and 2D simulations. *Fuel Process. Technol.* **2017**, *156*, 317–330. [[CrossRef](#)]
45. Yoon, I.; Shin, S. Maximal spreading of droplet during collision on particle: Effects of liquid viscosity and surface curvature. *Phys. Fluids* **2021**, *33*, 83310. [[CrossRef](#)]
46. Santolaya, J.L.; García, J.A.; Calvo, E.; Cerecedo, L.M. Effects of droplet collision phenomena on the development of pressure swirl sprays. *Int. J. Multiph. Flow* **2013**, *56*, 160–171. [[CrossRef](#)]
47. Ghahremani, A.R.; Saidi, M.H.; Hajinezhad, A.; Mozafari, A.A. Experimental investigation of spray characteristics of a modified bio-diesel in a direct injection combustion chamber. *Exp. Therm. Fluid Sci.* **2017**, *81*, 445–453. [[CrossRef](#)]
48. Ghahremani, A.R.; Jafari, M.; Ahari, M.; Saidi, M.H.; Hajinezhad, A.; Mozaffari, A.A. Spray characteristics and atomization behavior of bio-diesel (Norouzak) and diesel fuel blends. *Part. Sci. Technol.* **2018**, *36*, 270–281. [[CrossRef](#)]
49. Won, J.; Baek, S.W.; Kim, H.; Lee, H. The Viscosity and Combustion Characteristics of Single-Droplet Water-Diesel Emulsion. *Energies* **2019**, *12*, 1963. [[CrossRef](#)]
50. Ismael, M.A.; Heikal, M.R.; Aziz, A.R.; Crua, C.; El-Adawy, M.; Nissar, Z.; Baharom, M.B.; Zainal, A.E.Z. Firmansyah Investigation of Puffing and Micro-Explosion of Water-in-Diesel Emulsion Spray Using Shadow Imaging. *Energies* **2018**, *11*, 2281. [[CrossRef](#)]
51. You, C.; Zhao, H.; Cai, Y.; Qi, H.; Xu, X. Experimental investigation of interparticle collision rate in particulate flow. *Int. J. Multiph. Flow* **2004**, *30*, 1121–1138. [[CrossRef](#)]
52. Tonini, S.; Cossali, G.E. A novel formulation of multi-component drop evaporation models for spray applications. *Int. J. Therm. Sci.* **2015**, *89*, 245–253. [[CrossRef](#)]
53. Vysokomornaya, O.V.; Shlegel', N.E.; Strizhak, P.A. Interaction of Water Droplets in Air Flow at Different Degrees of Flow Turbulence. *J. Eng. Thermophys.* **2019**, *28*, 1–13. [[CrossRef](#)]
54. Volkov, R.S.; Kuznetsov, G.V.; Strizhak, P.A. Influence of droplet concentration on evaporation in a high-temperature gas. *Int. J. Heat Mass Transf.* **2016**, *96*, 20–28. [[CrossRef](#)]
55. Szakáll, M.; Urbich, I. Wind tunnel study on the size distribution of droplets after collision induced breakup of levitating water drops. *Atmos. Res.* **2018**, *213*, 51–56. [[CrossRef](#)]
56. Kuan, C.-K.; Pan, K.-L.; Shyy, W. Study on high-Weber-number droplet collision by a parallel, adaptive interface-tracking method. *J. Fluid Mech.* **2014**, *759*, 104–133. [[CrossRef](#)]
57. Almohammed, N.; Breuer, M. Towards a deterministic composite collision outcome model for surface-tension dominated droplets. *Int. J. Multiph. Flow* **2019**, *110*, 1–17. [[CrossRef](#)]
58. Ruan, C.; Xing, F.; Huang, Y.; Xu, L.; Lu, X. A parametrical study of the breakup and atomization process of two impinging liquid jets. *At. Sprays* **2017**, *27*, 1025–1040. [[CrossRef](#)]
59. Fathinia, F.; Khiadani, M.; Al-Abdeli, Y.M.; Shafieian, A. Performance improvement of spray flash evaporation desalination systems using multiple nozzle arrangement. *Appl. Therm. Eng.* **2019**, *163*, 114385. [[CrossRef](#)]
60. Liang, G.; Mudawar, I. Review of mass and momentum interactions during drop impact on a liquid film. *Int. J. Heat Mass Transf.* **2016**, *101*, 577–599. [[CrossRef](#)]
61. Liang, G.; Mudawar, I. Review of drop impact on heated walls. *Int. J. Heat Mass Transf.* **2017**, *106*, 103–126. [[CrossRef](#)]
62. Šikalo, Š.; Marengo, M.; Tropea, C.; Ganić, E.N. Analysis of impact of droplets on horizontal surfaces. *Exp. Therm. Fluid Sci.* **2002**, *25*, 503–510. [[CrossRef](#)]
63. Demidovich, A.V.; Kropotova, S.S.; Piskunov, M.V.; Shlegel, N.E.; Vysokomornaya, O.V. The Impact of Single- and Multicomponent Liquid Drops on a Heated Wall: Child Droplets. *Appl. Sci.* **2020**, *10*, 942. [[CrossRef](#)]
64. Clavijo, C.E.; Crockett, J.; Maynes, D. Hydrodynamics of droplet impingement on hot surfaces of varying wettability. *Int. J. Heat Mass Transf.* **2017**, *108*, 1714–1726. [[CrossRef](#)]
65. Negeed, E.-S.R.; Ishihara, N.; Tagashira, K.; Hidaka, S.; Kohno, M.; Takata, Y. Experimental study on the effect of surface conditions on evaporation of sprayed liquid droplet. *Int. J. Therm. Sci.* **2010**, *49*, 2250–2271. [[CrossRef](#)]
66. Fujimoto, H.; Tong, A.Y.; Takuda, H. Interaction phenomena of two water droplets successively impacting onto a solid surface. *Int. J. Therm. Sci.* **2008**, *47*, 229–236. [[CrossRef](#)]
67. Sen, S.; Vaikuntanathan, V.; Sivakumar, D. Impact dynamics of alternative jet fuel drops on heated stainless steel surface. *Int. J. Therm. Sci.* **2017**, *121*, 99–110. [[CrossRef](#)]
68. Fujimoto, H.; Yoshimoto, S.; Takahashi, K.; Hama, T.; Takuda, H. Deformation behavior of two droplets successively impinging obliquely on hot solid surface. *Exp. Therm. Fluid Sci.* **2017**, *81*, 136–146. [[CrossRef](#)]
69. Buck, B.; Tang, Y.; Deen, N.G.; Kuipers, J.A.M.; Heinrich, S. Dynamics of wet particle-wall collisions: Influence of wetting condition. *Chem. Eng. Res. Des.* **2018**, *135*, 21–29. [[CrossRef](#)]

70. Wang, B.; Ke, B.; Chen, B.; Li, R.; Tian, R. Study on the size of secondary droplets generated owing to rupture of liquid film on corrugated plate wall. *Int. J. Heat Mass Transf.* **2020**, *147*, 118904. [[CrossRef](#)]
71. Senda, J.; Kanda, T.; Al-Roub, M.; Farrell, P.V.; Fukami, T.; Fujimoto, H. Modeling Spray Impingement Considering Fuel Film Formation on the Wall. *SAE Tech. Pap.* **1997**, *106*, 98–112.
72. Roisman, I. Inertia dominated drop collisions. II. An analytical solution of the Navier–Stokes equations for a spreading viscous film. *Phys. Fluids* **2009**, *21*, 52104. [[CrossRef](#)]
73. Shayunusov, D.; Eskin, D.; Balakin, B.V.; Chugunov, S.; Johansen, S.T.; Akhatov, I. Modeling Water Droplet Freezing and Collision with a Solid Surface. *Energies* **2021**, *14*, 1020. [[CrossRef](#)]
74. Gelfand, B.E. Droplet breakup phenomena in flows with velocity lag. *Prog. Energy Combust. Sci.* **1996**, *22*, 201–265. [[CrossRef](#)]
75. Nasr, G.; Yule, A.; Bendig, L. *Industrial sprays and atomization: Design, analysis and applications*; Springer: London, UK, 2002.
76. Flock, A.K.; Guildenbecher, D.R.; Chen, J.; Sojka, P.E.; Bauer, H.-J. Experimental statistics of droplet trajectory and air flow during aerodynamic fragmentation of liquid drops. *Int. J. Multiph. Flow* **2012**, *47*, 37–49. [[CrossRef](#)]
77. Pilch, M.; Erdman, C.A. Use of breakup time data and velocity history data to predict the maximum size of stable fragments for acceleration-induced breakup of a liquid drop. *Int. J. Multiph. Flow* **1987**, *13*, 741–757. [[CrossRef](#)]
78. Shraiber, A.A.; Podvysotsky, A.M.; Dubrovsky, V. Deformation and breakup of drops by aerodynamic forces. *At. Sprays* **1996**, *6*, 667–692.
79. Wierzba, A. Deformation and breakup of liquid drops in a gas stream at nearly critical Weber numbers. *Exp. Fluids* **1990**, *9*, 59–64. [[CrossRef](#)]
80. Girin, G. On the mechanism of inviscid drop breakup at relatively small weber numbers. *At. Sprays* **2012**, *22*, 921–934. [[CrossRef](#)]
81. Guo, J.-P.; Wang, Y.-B.; Bai, F.-Q.; Zhang, F.; Du, Q. Effects of Asymmetric Gas Distribution on the Instability of a Plane Power-Law Liquid Jet. *Energies* **2018**, *11*, 1854. [[CrossRef](#)]
82. Chou, W.-H.; Faeth, G.M. Temporal properties of secondary drop breakup in the bag breakup regime. *Int. J. Multiph. Flow* **1998**, *24*, 889–912. [[CrossRef](#)]
83. Jackiw, I.M.; Ashgriz, N. On aerodynamic droplet breakup. *J. Fluid Mech.* **2021**, *913*, A33. [[CrossRef](#)]
84. Joseph, D.D.; Belanger, J.; Beavers, G.S. Breakup of a liquid drop suddenly exposed to a high-speed airstream. *Int. J. Multiph. Flow* **1999**, *25*, 1263–1303. [[CrossRef](#)]
85. Voytkov, I.S.; Kuznetsov, G.V.; Strizhak, P.A. The critical atomization conditions of high-potential fire suppressant droplets in an air flow. *Powder Technol.* **2021**, *384*, 505–521. [[CrossRef](#)]
86. Soni, S.K.; Kirar, P.K.; Kolhe, P.; Sahu, K.C. Deformation and breakup of droplets in an oblique continuous air stream. *Int. J. Multiph. Flow* **2020**, *122*, 103141. [[CrossRef](#)]
87. Kalogirou, S.A. Seawater desalination using renewable energy sources. *Prog. Energy Combust. Sci.* **2005**, *31*, 242–281. [[CrossRef](#)]
88. Romero, R.J.; Rodríguez-Martínez, A. Optimal water purification using low grade waste heat in an absorption heat transformer. *Desalination* **2008**, *220*, 506–513. [[CrossRef](#)]
89. Kuznetsov, G.V.; Strizhak, P.A.; Volkov, R.S.; Zhdanova, A.O. Amount of water sufficient to suppress thermal decomposition of forest fuel. *J. Mech.* **2020**, *33*, 703–711. [[CrossRef](#)]
90. Suzuki, Y.; Harada, T.; Watanabe, H.; Shoji, M.; Matsushita, Y.; Aoki, H.; Miura, T. Visualization of aggregation process of dispersed water droplets and the effect of aggregation on secondary atomization of emulsified fuel droplets. *Proc. Combust. Inst.* **2011**. [[CrossRef](#)]
91. Watanabe, H.; Harada, T.; Matsushita, Y.; Aoki, H.; Miura, T. The characteristics of puffing of the carbonated emulsified fuel. *Int. J. Heat Mass Transf.* **2009**, *52*, 3676–3684. [[CrossRef](#)]
92. Strizhak, P.A.; Piskunov, M.V.; Volkov, R.S.; Legros, J.C. Evaporation, boiling and explosive breakup of oil–water emulsion drops under intense radiant heating. *Chem. Eng. Res. Des.* **2017**, *127*, 72–80. [[CrossRef](#)]
93. Kuznetsov, G.V.; Piskunov, M.V.; Strizhak, P.A. Evaporation, boiling and explosive breakup of heterogeneous droplet in a high-temperature gas. *Int. J. Heat Mass Transf.* **2016**, *92*, 360–369. [[CrossRef](#)]
94. Meng, K.; Wu, Y.; Lin, Q.; Shan, F.; Fu, W.; Zhou, K.; Liu, T.; Song, L.; Li, F. Microexplosion and ignition of biodiesel/ethanol blends droplets in oxygenated hot co-flow. *J. Energy Inst.* **2019**, *92*, 1527–1536. [[CrossRef](#)]
95. Hou, S.-S.; Rizal, F.M.; Lin, T.-H.; Yang, T.-Y.; Wan, H.-P. Microexplosion and ignition of droplets of fuel oil/bio-oil (derived from lauan wood) blends. *Fuel* **2013**, *113*, 31–42. [[CrossRef](#)]
96. Hoxie, A.; Schoo, R.; Braden, J. Microexplosive combustion behavior of blended soybean oil and butanol droplets. *Fuel* **2014**, *120*, 22–29. [[CrossRef](#)]
97. Wang, C.H.; Hung, W.G.; Fu, S.Y.; Huang, W.C.; Law, C.K. On the burning and microexplosion of collision-generated two-component droplets: Miscible fuels. *Combust. Flame* **2003**, *134*, 289–300. [[CrossRef](#)]
98. Palazzo, N.; Zigan, L.; Huber, F.J.T.; Will, S. Impact of Oxygenated Additives on Soot Properties during Diesel Combustion. *Energies* **2021**, *14*, 147. [[CrossRef](#)]
99. Wang, C.H.; Liu, X.Q.; Law, C.K. Combustion and microexplosion of freely falling multicomponent droplets. *Combust. Flame* **1984**, *56*, 175–197. [[CrossRef](#)]
100. Li, S.; Zhang, Y.; Qi, W.; Xu, B. Quantitative observation on characteristics and breakup of single superheated droplet. *Exp. Therm. Fluid Sci.* **2017**, *80*, 305–312. [[CrossRef](#)]
101. Law, C.K. Internal boiling and superheating in vaporizing multicomponent droplets. *AIChE J.* **1978**, *24*, 626–632. [[CrossRef](#)]

102. Sazhin, S.S.; Rybdylova, O.; Crua, C.; Heikal, M.; Ismael, M.A.; Nissar, Z.; Aziz, A.R.B.A. A simple model for puffing/micro-explosions in water-fuel emulsion droplets. *Int. J. Heat Mass Transf.* **2019**, *131*, 815–821. [[CrossRef](#)]
103. Antonov, D.V.; Piskunov, M.V.; Strizhak, P.A. Breakup and explosion of droplets of two immiscible fluids and emulsions. *Int. J. Therm. Sci.* **2019**, *42*, 30–41. [[CrossRef](#)]
104. Antonov, D.V.; Piskunov, M.V.; Strizhak, P.A. Explosive disintegration of two-component drops under intense conductive, convective, and radiant heating. *Appl. Therm. Eng.* **2019**, *152*, 409–419. [[CrossRef](#)]
105. Kuznetsov, G.V.; Shlegel, N.E.; Solomatin, Y.; Strizhak, P.A. Combined techniques of secondary atomization of multi-component droplets. *Chem. Eng. Sci.* **2019**, *209*, 115199. [[CrossRef](#)]
106. Davanlou, A.; Lee, J.D.; Basu, S.; Kumar, R. Effect of viscosity and surface tension on breakup and coalescence of bicomponent sprays. *Chem. Eng. Sci.* **2015**, *131*, 243–255. [[CrossRef](#)]